follows. Firstly, the HAp fibers were synthesized from aqueous solutions in the $Ca(NO_3)_2$-$(NH_4)_2HPO_4$-$(NH_2)_2CO$-HNO_3 system [4]. The HAp fibers were suspended with spherical carbon beads (Nika beads; Nihon Carbon Company) with a diameter of ~150 μm in the mixed solvent (ethanol/water=1/1(v/v)). The carbon beads were added to the HAp fiber in the following carbon/HAp (w/w) ratios: 20/1, 10/1, 1/1 and 0/1.

The green compacts for the scaffold were fabricated by pouring and vacuum pumping the above mixed suspension containing ~1 mass % of the HAp (5 cm^3) into the vinyl-chloride mould of 16.5 mm in internal diameter. The resulting compacts were fired at 1300°C for 5 h in a steam atmosphere to develop the structure of the scaffold. Hereafter, we name the scaffolds derived from carbon/HAp= 20/1, 10/1 and 0/1 (w/w) "AFS2000", "AFS1000" and "AFS0", respectively.

The resulting scaffolds were characterized as follows: i) phase identification by X-ray diffractometry (XRD) and infrared spectroscopy (IR), ii) observation of microstructure by scanning electron microscopy (SEM), iii) examination of pore size distribution by mercury porosimetry and iv) measurement of porosity on the basis of the mass and dimension of the scaffolds.

Biological evaluation of AFS using MC3T3-E1 cells

The resulting scaffolds were biologically evaluated using osteoblastic cells, MC3T3-E1 [6]. The cellular responses to the three kinds of scaffolds, AFS0, AFS1000 and AFS2000, were examined by observing i) the initial cell-attachment efficiency after seeding for 5 h, ii) the cell proliferation during 1 to 21 d, iii) gene expressions of differentiation makers of osteoblasts (7 and 21 d), iv) the cell morphology.

Five hundred thousand cells were seeded on each scaffold and cultured for the desired period of time. The medium used was α-minimum essential medium (α-MEM) with 10% fetal bovine serum (FBS) (Gibco BRL); culture conditions were at 37 °C in a 5% CO_2 atmosphere.

As for initial cell-attachment efficiency and proliferation, the DNA contents in the cell cultured with 3D scaffolds were measured instead of usual cell-counting. DNA contents were determined using the Hoechst 33258 method. Cell morphology was observed using SEM after fixation by a 10% gultaraldhyde solution at 4 °C for 1 h.

Gene expressions of the cell cultured with AFSs were examined by the reverse-transcription polymerase chain reaction (RT-PCR) method (7, 21 d). Total RNA of the cells was extracted using TRIZOL® (Gibco BRL) regent. Complementary DNA (cDNA) was prepared by reverse transcription of the mRNA. Expression of differentiation maker genes, that is, I-collagen (I-col), alkaline phosphatase (ALP), osteopontin (OP), and bone sialoprotein (BSP), of osteoblasts were examined by electrophoresis of the PCR products obtained from the reactions of cDNA with some primers.

Biological evaluation of AFS using Rat bone marrow cells (RBMC)

The resulting scaffolds were also biologically evaluated using bone marrow cells derived from the wistar rats (4 weeks old, male), as reported by Maniatopoulos *et al.* [7]. In the RBMC cases, the cell differentiation and calcification were especially examined. The contents of the ALP and osteocalcin (OC) in the cell cultured with AFSs were determined for clarifying the stages of cell differentiation.

Five hundred thousand cells were seeded on each scaffold and cultured for the desired period of time. The medium used was α-MEM with 10% FBS containing 10 nM dexamethazone, 200 μM ascolbic acid and 1 mM β-sodium glycerophosphate; culture conditions were 37 °C in a 5% CO_2 atmosphere.

The ALP activity was determined by normalizing for DNA content in the cell cultured as early to middle stage of osteoblast differentiation. The ALP assays were measured using a kit of Wako chemicals based on the Bessey-Lowry method and polystyrene plate for cell culture was used as a control.

The OC contents were also determined by normalizing for DNA content as the last stage of osteoblast differentiation. The OC were assayed using a kit of Takara based on the ELIZA method and polystyrene plate for cell culture was used as a control.

Results and Discussion

Characterization of AFSs for cell-culture testing

Table 1 shows the preparation conditions of typical scaffolds and their porosity and median pore size. Single HAp phase was present in the resulting scaffolds regardless of carbon-bead addition. The HAp had preferred orientation in the (h00) planes: (100), (200) and (300). The porosities of the AFSs increased from ~94% to ~99% as the volume fraction of carbon beads was increased.

Figure 1 shows the microstructure of the AFS0 (a) and AFS2000 (b). The SEM observation showed that the AFS2000 scaffold was composed of large pores of 100-300 μm in diameter and smaller pores formed by intertwining of individual fibers and that the pores were

Table 1 Some properties of the AFSs.

Sample name	Carbon/HAp [w/w]	Porosity [%]	Median pore size [μm]
AFS0	0/1	94±0.5	5.2
AFS1000	10/1	98±0.1	112.8
AFS2000	20/1	99±0.1	247.3

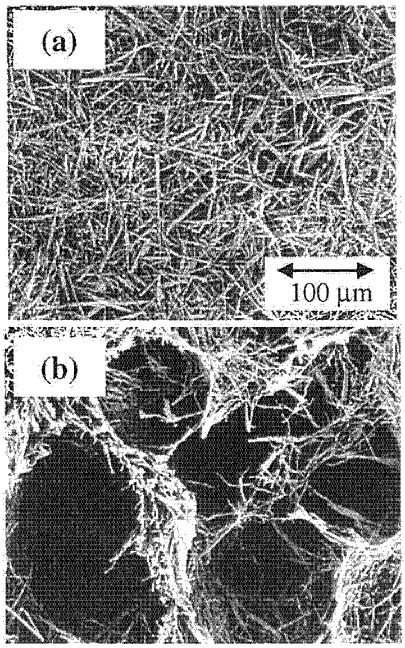

Fig. 1 Microstructure of (a) AFS0 and (b) AFS2000.

interconnected in the structure. As compared with microstructure of the carbon-free derived scaffold (AFS0), the pore sizes of the scaffolds, AFS1000 (data not shown) and AFS2000, were significantly enlarged with increasing amounts of the carbon beads added.

The pore-size distribution of the scaffolds was measured using a mercury porosimeter. The median pore sizes are listed in Table 1. In the case of the AFS0 scaffold, the pore size distribution was very limited; in the range of about 5 μm. On the other hand, the pore size distribution of the AFS2000 scaffold shifted toward larger pore sizes, that is, in the range of 100-500 μm. In particular, the AFS2000 scaffold may contain pores of dimensions suitable for cell in-growth.

In vitro biological evaluation of the AFSs

We firstly performed a biological evaluation using MC3T3-E1 cells. The initial cell-attachment efficiency cultured on/in the specimens was 74.2±1.5 % for control (24 well cell-culture plate; polystyrene), 55.0±1.9 % for the AFS0 and 96.2±4.5 % for the AFS2000. The AFS2000 showed the highest value among the examined specimens.

Figure 2 shows the growth curves of the cells seeded on these three kinds of sample. The cells in the AFS2000 proliferated in a similar manner to those on the control and the AFS0 during the incubating periods from 1 d up to 7 d. However, the cells in the AFS2000 proliferated more than those in the AFS0 and on the control after the long incubating periods of 7 d to 21 d. The present good cell proliferation results may be due to the 3D structure of the AFS2000.

The SEM observation of the cells cultured for 21 d revealed that the AFS2000 scaffold was able to support 3D cell proliferation more efficiency, compared with AFS0 (data not shown).

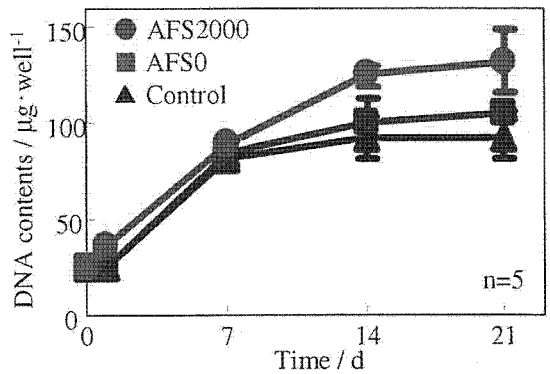

Fig. 2 Proliferation of cells cultured in/on the scaffolds.

The results of differentiation of cells cultured in AFSs are shown in Fig. 3, together with those of control. We chose the four proteins: I-Col, ALP, OP and BSP, as the differentiation markers. In the case of AFS2000, the amplified fragment of ALP cDNA was observed after culture for 7 d, and then that of the BSP after culture for 21 d, although the latter band was not clear. This finding reveals that AFS2000 will promote the differentiation of osteoblast.

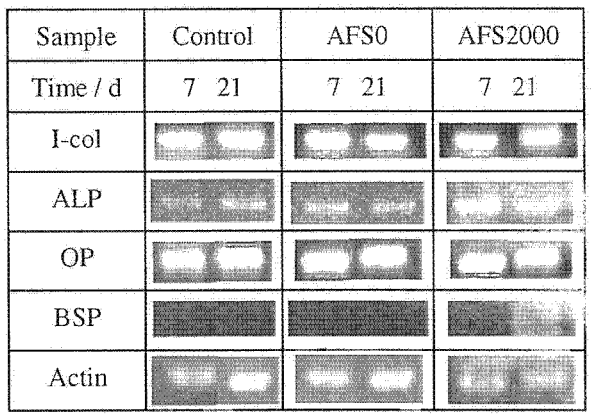

Fig. 3 Gene expression of the specific proteins of the cells cultured in/on the AFSs using actin as a control.

Next, biological evaluation using rat bone marrow cells was performed to examine the differentiation of the cells into osteoblasts and subsequent calcification leading to bone regeneration.

Figure 4 shows the ALP activity normalized for the DNA content of the cells cultured on/in scaffolds for 7, 14 and 28 d. The ALP activity of the AFS2000 showed the highest value amongst the tested samples. These results could be regarded as significant ($P<0.05$) by ANOVA. The ALP activity of the cells cultured on the control decreased at 14 and 21 d. Although the ALP activity of the cells cultured in the AFS0 attained the maximum value at 14 d, the value decreased at 21 d. In the case of the AFS2000, the ALP activity increased with longer incubating periods. This may be the reason why the AFS2000 scaffold with high porosity and large pore size provided the most suitable environment for enhancing bone marrow cell activity.

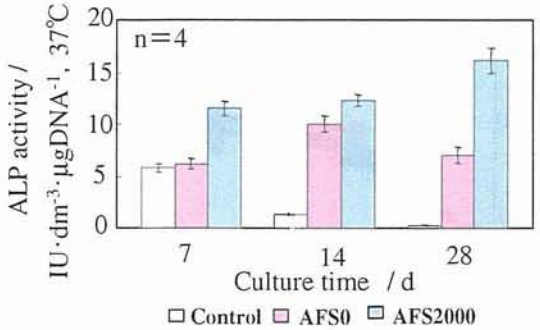

Fig. 4 ALP activity normalized for DNA content of the cells cultured in/on the AFSs.

Contents of the OC normalized for the DNA content was also determined as illustrated in Fig. 5. This finding that the AFS2000 has given the best result with respect to all the tests demonstrate that the high porosity and large pore size fulfilled by the AFS2000 could provide an excellent environment for enhancing bone marrow cell activity.

In addition, Morisue and Matsumoto have recently reported on rat model of posterolateral spinal fusion that the current AFS is clinically effective as a carrier of rh-BMP-2 for bone regeneration [8]. Based on the findings from *in vitro/vivo* evaluations, the AFS2000 scaffolds may be effective as the matrix for tissue engineering, leading to bone regeneration.

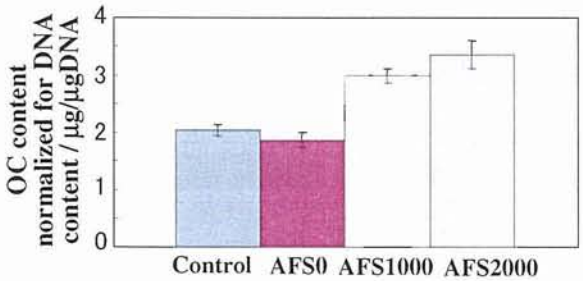

Fig. 5 OC contents normalized for DNA content of the cells cultured for 28 d in/on the AFSs (sample: n=4).

Conclusion

Novel scaffolds for tissue engineering for bone have been developed from single-crystal apatite fibers synthesized by a homogeneous precipitation method. The resulting AFSs have large pores of 110-250 μm in diameter and high porosities of 98-99%. The scaffolds were biologically evaluated using two kinds of cells, MC3T3-E1 and RBMC. In both cases, the cells cultured on/in the scaffolds showed excellent cellular responses, such as good cell proliferation and enhanced differentiation into osteoblasts. Especially, the AFS2000 was able to support 3D cell proliferation. We conclude that the AFS2000 scaffolds with high porosity and large pore size may be effective as the matrix for tissue engineering leading to bone regeneration.

Acknowledgement

A part of the present research has been defrayed by the Industrial Technology Research Grant Program in 2002-04 from NEDO (New Energy and Development Organization), and ''Academic Frontier'' Project for Private Universities: matching fund subsidy from MEXT (Ministry of Education, Culture, Sports, Science and Technology), 2006-2010.

References

[1] Ogushi H. (2002): "Bone tissue regeneration using marrow mesenchymal stem cells and ceramics – From basic science to clinical application –", *J. Jpn. Soc. Biomater.*, **20**, pp. 296-304.

[2] Aizawa M., Shinoda H., Uchida H., Itatani K., Okada I., Matsumoto M., Morisue H., Matsumoto H., and Toyama Y. (2003): "Development and Biological Evaluation of Apatite Fiber Scaffolds with Large Pore Size and High Porosity for Bone Regeneration", *Key Engineer. Mater*, **240-242**, pp. 647-650.

[3] Aizawa M., Shinoda H., Uchida H., Okada I., Fujimi T. J., Kanzawa N., Morisue H., Matsumoto M., and Toyama Y. (2004): "*In Vitro* Biological Evaluations of Three-Dimensional Scaffold Developed from Single-crystal Apatite Fibres for Tissue Engineering of Bone", *Phosphorus Res. Bull.*, **17**, pp. 268-273.

[4] Aizawa M., Porter A. E., Best S. M., and Bonfield W., (2005): "Ultrastructural Observation of Single-crystal Apatite Fibres", *Biomaterials*, **26**, pp. 3427-3433.

[5] Aizawa M., Ueno H., and Okada I. (2003): "Development of Scaffolds for Tissue Engineering Using Single-crystal Apatite Fibres and Their Biological Evaluation by Osteoblastic Cell", *Trans. Mater. Res. Soc. Jpn.*, **28**, pp. 849-852.

[6] Sudo H., Kodama H., Amagai Y., Yamamoto S. and Kasai S. (1983): '*In Vitro* differentiation and calcification in a new clonal osteogenic cell line derived from newborn mouse calvaria', *J. Cell Biol.*, **96**, pp. 191-198.

[7] Maniatopoulos C., Sodek J. and Melcher, A. H. (1988): "Bone formation in vitro by stromal cells obtained from bone marrow of young adult rats", *Cell Tissue Res.*, **254**, pp. 317-330.

[8] Morisue H., Matsumoto M., Chiba K., Matsumoto H., Toyama Y., Aizawa M., Kanzawa N., Fujimi T. J., Uchida H., Okada I. (2006): "A novel hydroxyapatite fiber mesh as a carrier for recombinant human bone morphogenetic protein-2 enhances bone union in rat posterolateral fusion model", *Spine*, **31**, pp. 1194-200.

OSTEOGENIC DIFFERENTIATION IN A THREE-DIMENSIONAL APATITE-FIBER SCAFFOLD

Michiyo Honda[1*], Takahiko J. Fujimi[1], Nobuyuki Kanzawa[1], Koji Izawa[1], Takahide Tsuchiya[1], Mamoru Aizawa[2],

[1] Department of Chemistry, Faculty of Science and Engineering, Sophia University, Tokyo, Japan
[2] Department of Applied Chemistry, School of Science and Technology, Meiji University, Kanagawa, Japan

* Corresponding Author E-Mail Address: honda-m@sophia.ac.jp

Abstract: Osteogenic differentiation of MC3T3-E1 cells in a three-dimensional (3-D) scaffold has been studied in this work. We examined the expression of bone-related genes during differentiation of MC3T3-E1 cells in a 3-D culture system. To evaluate the relevance of 3-D culture environment to osteogenic differentiation, we compared two distinct carriers. We used the tissue culture plate for 2-D culture and Apatite-Fiber Scaffold (AFS) for 3-D culture. The AFS-formed 3-D network of fibers had a high porosity and two different sizes of pores.
Culturing cells in the AFS resulted in increases in mRNA expression level of type I collagen, osteocalcin and osteopontin in the absence of dexamethasone at 4, 7 , 14 and 21 days compared with those in the 2-D culture. Additionally, in the AFS those bone-related genes expressed earlier than in 2-D culture and started osteogenic differentiation. These results demonstrated that AFS had the 3-D culture system enhanced osteogenic differentiation. We thought AFS facilitated the cell proliferation and the cell differentiation by using two different pores properly. We concluded that this characteristic structure of AFS was one of the essential factors for osteogenic differentiation.

Introduction

The need to repair defects in bone is a significant problem faced by orthopaedic medicine. Tissue engineering and regenerative medicine offer solutions to a number of clinical problems that have not been adequately addressed through the use of permanent replacement devices [1]. At present, the cell tissue devices that function as an alternative organization and internal organs are developed by using the cell culture technology to achieve new management that takes the place of the organ transplantation. Tissue engineering has been used to enhance the utility of biomaterials for clinical bone repair by the incorporation of an osteogenic cell source into a scaffold followed by the *in vitro* promotion of osteogenic differentiation before host implantation [2]. As the first step, it is necessary to culture a large amount of target cells for an anagenesis. However, the organization with the function cannot be regenerated by a conventional, two-dimensional culture. The culture space arranged in three dimensions is necessary for the ideal cell culture, because cells are proliferated and differentiated *in vivo* in a three-dimensional environment. Appropriate pore size and porosity are necessary for the three-dimensional cell extension; in this context, most studies were carried out in the 2-D culture system to understand the changes in molecular events observed during the cell differentiation. However, 3-D cellular development is essential for *in vitro* bone formation [3, 4]. *In vitro* osteoblast differentiation in the 3-D culture system may be more closely relevant to the *in vivo* bone formation process. Apatite-fiber scaffold (AFS) with high porosity and excellent biocompatibility has been developed based on such clinical demand [5].

The aim of this study is to investigate the cell compatibility and the ability of high-density cell culture in the AFS and to evaluate the relevance of 3-D culture environment to osteogenic differentiation. The present study revealed that 3-D culture system was effective to regulate cell proliferation and differentiation similar to the situation *in vivo*.

Materials and Methods

Fabrication process of apatite-fiber scaffold and its characterization

The hydroxyapatite (HAp) fibers were prepared from aqueous solutions in the $Ca(NO_3)_2$-$(NH_4)_2HPO_4$-$(NH_2)_2CO$-HNO_3 system through a homogeneous precipitation method using urea, as previously reported [5,6]. The HAp fibers were suspended with spherical carbon beads (Nika beads; Nihon Carbon Company) with a diameter of ~150 μm in the mixed solvent (ethanol/water=1/1(v/v)). The carbon beads were added to the HAp fiber at a ratio of carbon/HAp (w/w): 20/1. The green compacts for the scaffold were fabricated by pouring and vacuum pumping the above mixed suspension containing ~1 mass % of the HAp (5 cm^3) into a vinylchloride mould of 16.5 mm in internal diameter. The resulting compacts were fired at 1300°C for 5 h in a steam atmosphere to develop the structure of the scaffold. The resulting scaffolds were characterized as follows: i) phase identification by X-ray diffractometry (XRD) and infrared spectroscopy (IR),

ii) observation of microstructure by scanning electron microscopy (SEM), iii) examination of pore size distribution by mercury porosimetry and iv) measurement of porosity on the basis of the mass and dimension of the scaffolds.

Cell culture

MC3T3-E1 preosteoblasts were cultured in a regular culture medium consisting of α-modified minimum essential medium (α-MEM; Sigma) supplemented with 10% heat-inactivated fetal bovine serum (FBS; Sigma) in a humidified atmosphere of 5% CO_2 at 37°C [7]. Before the experiments, MC3T3-E1 cells were trypsinized and plated onto two different carriers at a density of 2×10^6 cells/mL, and cultured in regular media or osteogenic media (regular media described above plus 10 nM dexamethasone (DEX), 1 mM β-glycerol phosphate and 200 μM ascorbic acid) before they were harvested at 4, 7, 14 and 21 days.

RNA isolation and quantative real-time RT-PCR

The gene expression of MC3T3-E1 cells-cultured on two different carriers in osteogenic media was determined by RNA isolation followed by real-time RT-PCR. To investigate the potential of AFS to induce osteoblastic gene expression in the absence of known inductive agent, we also cunducted an additional experiment in which MC3T3-E1 cells were cultured in regular media. After 4, 7, 14 and 21 days, total RNA was isolated using TRIZOL® (Invitrogen) reagent. RNA was reverse-transcribed using dT primers and M-MLV reverse trascriptase (Takara). To evaluate the expression level of type I collagen (I-col), osteopontin (OP) and osteocalcin (OC), we used QuantiTect SYBR Green RT-PCR (Qiagen) according to the manufacturer's instructions. The expression level of all osteogenic markers was normalized to the house-keeping gene, glyceraldehydes 3-phosphate dehydrogenase (GAPDH). Primers were as follows: *I-col*: forward primer, 5'-TCC TGGGCCTATCTGATCTC-3'; reverse primer, 5'-TTG ATGCAGGACAGACCAAGA-3'. *OP*: forward primer, 5'- CGATTACACTTTCACTCCAATCG-3'; reverse primer, 5'-CAGTCCATAAGCCAAGCTATCA-3'. *OC*: forward primer, 5'-GAGGACAGGGAGGATCAA GTC-3'; reverse primer, 5'- GACCTGTGCTGCCCTA AAGC-3'. *GAPDH*: forward primer, 5'-TGGATGCAG GGATGATGTTC-3'; reverse primer, 5'-ACTGCCAC CCAGAAGACTGT-3'.

Immunofluorescence microscopy

MC3T3-E1 cells were grown on AFS for 7 days in regular media or osteogenic media. AFS after culturing cells were fixed with 3.5% paraformaldehyde/PBS, immersed in 1% gelatin, and embedded in O.C.T. compound (Sakura Tissue-Tek). Thin sections (approximately 20-μm thickness) were reacted with Alexa Fluor®594-labelled phalloidin (Molecular Probes Inc.) or OP or OC antibody. Fluorescence images were examined by confocal laser scanning microscopy (Zeiss).

Results

Distribution of MC3T3-E1 cells in AFS

In order to investigate the cell distribution in the 3-D culture system, we used AFS that has a high porosity (~99%) and two different sizes of pores. The medium pore sizes of ~5 μm are called micro-pores, and the others of ~250 μm are called macro-pores. The size of the micro-pores is too small to culture the cells three-dimensionally; however, macro-pores are suitable to culture the cells three dimensionally. At 7 days after culture in regular media, thin sections were stained with Alexa Fluor®594 labelled phalloidin. We observed that the cells were unified with a frame of AFS closely. And the cells extended and formed bridges within macro- and micro-pores (Fig. 1). This indicated that MC3T3-E1 cells adhered to carriers not only two-dimensionally, but also distributed three-dimensionally in the AFS.

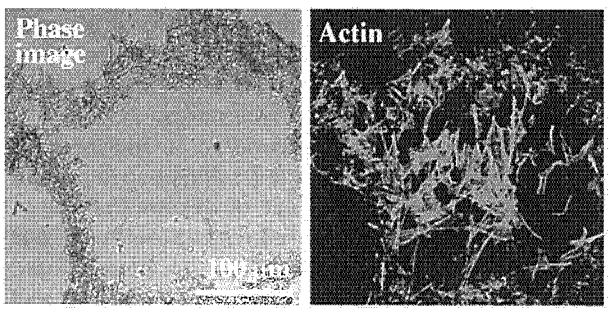

Fig. 1 Distribution of MC3T3-E1 cells in AFS.

Osteogenic differentiation of MC3T3-E1 cultured in the 2-D and 3-D system

Previous studies have shown that MC3T3-E1 cells which were cultured in the 3-D system (AFS2000) expressed bone markers such as I-col, ALP, OP and BSP, and have suggested that AFS2000 would promote the differentiation of osteoblast [5].

To evaluate the relevance of the 3-D culture environment to osteogenic differentiation, we cultured cell on/in the tissue culture plate or AFS. Additionally, to investigate the potential of AFS to induce osteoblastic gene expression, we cultured cells in regular media or osteogenic media. At 4, 7, 14 and 21 (only AFS) days after seeding, we have analyzed the expression pattern of bone-related genes including I-col, OP and OC in detail using quantitative real-time RT-PCR. We have tried to extract total RNA from the cells which were cultured in the 2-D plate after 21-days seeding; however, mineralization has made it difficult to extract RNA. In both media (regular and osteogenic media), differences were seen in the expression pattern of markers between culture plate and AFS. As for I-col, AFS let the expression level increase immediately by 4 days after seeding in regular media. On the other hand, in the plate, I-col expression exhibited a slight increase until 7 days

(Fig. 2A). In both carriers the expression level of I-col was decreased as a culture period passed. Almost the same expression pattern was observed in osteogenic media, even if there was a difference in the quantity ratio (data not shown). We also found a significant increase in OP expression during a 2-week period in regular media in the AFS, though the expression of OP in the culture plate was lower than that of AFS (data not shown). These findings show that AFS has the ability for differentiation compared to the culture plate until the middle of differentiation. In the case of OC, the expression level increased rapidly in the culture plate from 7 to 14 days. On the other hand, OC expression in the AFS remained unchanged within 14 days after seeding, and a significant increase was observed at 21 days (Fig. 2B). Thus, it was necessary for long term culture to detect the high expression level of OC in AFS.

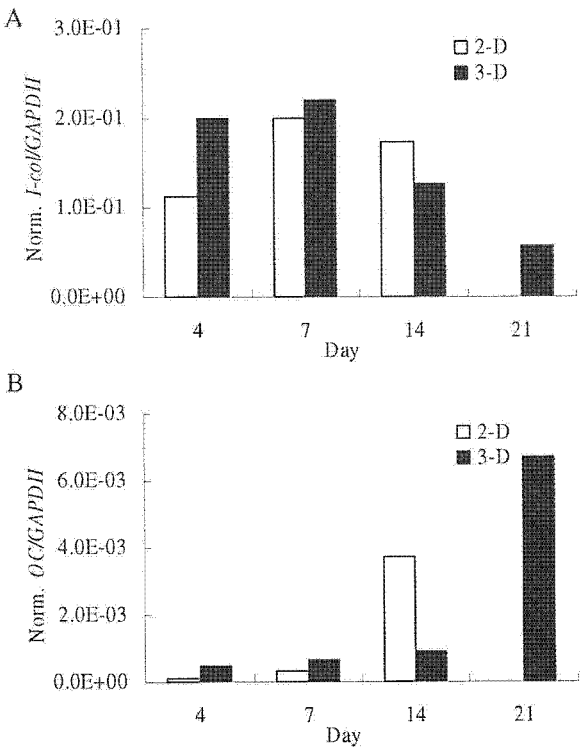

Fig. 2 Comparison of osteoblastic gene expressions in culture plate and AFS with regular media.

Immunodetection of marker proteins in AFS

To clarify the osteogenic differentiation in AFS, we performed immunocytochemistry with using marker proteins. After 7-days culture in regular media, thin sections were reacted with either anti-OP or -OC antibody. The signals for OP were detected strongly within micro-pores (Fig. 3); however, those of OC were too weak to detect such signals (data not shown). Cells that penetrated into the micro-pore in high density seem to start the cell differentiation and express OP; however, they did not differentiate enough so as to express the OC that is a marker of the latest stage of differentiation. These data were consistent with those of real-time PCR, indicating that bone differentiation was generated in micro-pores preferentially.

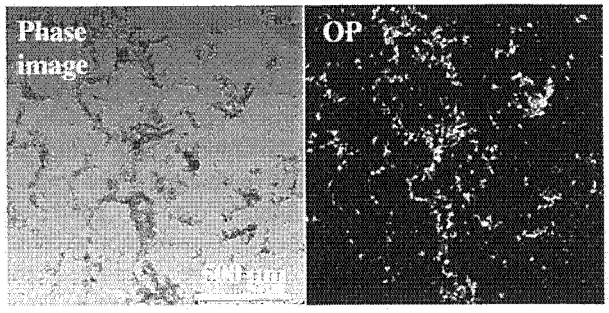

Fig. 3 Localization of OP in the AFS.

Discussion

The 3-D culture system facilitates the construction and development of functioning tissue units within the scaffolds that mimic the biological and mechanical function [3]. The 3-D culture system might be conducive to regulate cell proliferation and differentiation similar to the situation *in vivo*. Thus, AFS which is able to culture cells in three dimension is thought to provide a suitable environment for cell expansion and differentiation.

In this study, we showed how the structure feature contributes to the promotion of osteogenic differentiation by comparing the AFS with two-dimensional culture plates. The observation of cell distributions in AFS with two different sizes of pores showed that cells bridged within macro-pores for three dimensions. And we have also observed the cells that entered in micro-pores, and came in close contact with the apatite fibers. The environment to which the cells are filled in a high density is thought to work advantageously for the cell differentiation. Thus, macro-pores seem to support the cell growth and proliferation, and micro-pore facilitates cell differentiation. In fact, the results of real-time RT-PCR suggested that the structure of AFS affected the facilitation of differentiation. It is conceivable that this specific environment of AFS may induce MC3T3-E1 cells to switch from a proliferative state to more differentiated state at micro-pores. Finally, fully grown cells in macro-pores were differentiated a higher extent than that cultured in two dimensional plates. Additionally, it has been reported that surface roughness, micro- and nano topography, can affect cell morphology, cytoskeleton, spreading, proliferation and differentiation [8]. Thus, the fine structure of the carrier is one of the important factors that influence various phenomena of the cells. The result that bone-related genes expressed earlier in the AFS than in the culture plate may reflect the complex structure constructed with fine apatite fibers where cells are attached to or surround fibers three-dimensionally. It is thought that AFS is an excellent carrier which is able to make proliferation and differentiation progress by using the pores with two different sizes properly.

Previous studies proposed that the inorganic ceramics have not shown osteoinductive ability, but they certainly possess osteoconductive abilities as well as a remarkable ability to bind bo ne directly [9]. This

opinion was different slightly from our result. However, the difference between our findings and previous studies may be explained by the structure of AFS. The single crystal apatite fibers may grow along the *c*-axis to develop the *a*(*b*)-plane of the hexagonal HAp. Thus, the apatite fibers may have a positive charge on the surface [5]. This orientation is thought to be good for biocompatibility and to produce an osteoinductive effect.

In the present study, we have evaluated the osteogenic differentiation only in a short period. Thus, long-term evaluation is necessary to examine molecular mechanism, and it will prove the usefulness of AFS for the bone tissue engineering.

Conclusions

In the present study, we evaluated the relevance of 3-D culture environment to osteogenic differentiation by comparing AFS with culture plates. The results showed that culture in AFS allowed 3-D distribution of MC3T3-E1 cells and enhanced cell-matrix interactions. Additionally, the expression of bone-related genes in AFS was earlier than in culture plates. And culturing cells in AFS resulted in increases in mRNA expression level of bone markers in regular media compared with those of in the culture plate. This indicated that AFS promoted the osteogenic differentiation using characteristic structure and that 3-D structure educed osteoinductive ability.

The spatial microenvironment in 3-D culture played an important role in promoting osteogenesis. This 3-D culture system can be used as an *in vitro* model to study osteoblast behaviour, and to understand molecular mechanisms.

References

[1] Spector M. (2006): 'Biomaterials-based tissue engineering and regenerative medicine solutions to musculoskeletal problems', *Swiss.Med.Wkly.*, **136**, pp. 293-301

[2] Mauney J.R., Blumberg J., Pirun M., Volloch V., Vunjak-Novakovic G., and Kaplan D.L. (2004): 'Osteogenic differentiation of human bone marrow stromal cells on partially demineralized bone scaffolds in vitro', *Tissue Eng.*, **10**, pp. 81-92

[3] Panoskaltsis N., Mantalaris A., and Wu J.H. (2005): 'Engineering a mimicry of bone marrow tissue ex vivo', *J.Biosci.Bioeng.*, **100**, pp. 28-35

[4] Huang W., Carlsen B., Wulur I., Rudkin G., Ishida K., Wu B., Yamaguchi D.T., and Miller T.A. (2004): 'BMP-2 exerts differential effects on differentiation of rabbit bone marrow stromal cells grown in two-dimensional and three-dimensional systems and is required for in vitro bone formation in a PLGA scaffold', *Exp.Cell Res.*, **299**, pp. 325-334

[5] Aizawa M, Shinoda H, Uchida H., Okada I., Fujimi T. J., Kanzawa N., Morisue H., Matsumoto M. and Toyama Y. (2004): '*In Vitro* Biological Evaluations of Three-Dimensional Scaffold Developed from Single-crystal Apatite Fibres for Tissue Engineering of Bone', *Phosphorus Res. Bull.*, **17**, pp. 268-273

[6] M. Aizawa, A. E. Porter, S. M. Best and W. Bonfield, "Ultrastructural Observation of Single-crystal Apatite Fibres", *Biomaterials*, **26**, 3427-3433(2005).

[7] Sudo H., Kodama H.A., Amagai Y., Yamamoto S., and Kasai S. (1983): 'In vitro differentiation and calcification in a new clonal osteogenic cell line derived from newborn mouse calvaria', *J.Cell Biol.*, **96**, pp. 191-198

[8] Chou Y.F., Huang W., Dunn J.C., Miller T.A., and Wu B.M. (2005): 'The effect of biomimetic apatite structure on osteoblast viability, proliferation, and gene expression', *Biomaterials*, **26**, pp. 285-295

[9] Burg K.J., Porter S., and Kellam J.F. (2000): 'Biomaterial developments for bone tissue engineering', *Biomaterials*, **21**, pp. 2347-2359

APATITE-FIBER SCAFFOLD PROVIDES THREE-DIMENSIONAL CULTURE ENVIRONMENT FOR OSTEOBLAST-LIKE CELLS

Shigeki Izumi[1], Michiyo Honda[1], Nobuyuki Kanzawa[1*], Takahiko J. Fujimi[1], Hiroshi Uchida[1], Takahide Tsuchiya[1], Hikaru Morisue[2], Morio Matsumoto[2], Mamoru Aizawa[3]

[1] Department of Chemistry, Faculty of Science and Technology, Sophia University, Tokyo, Japan
[2] Department of Orthopaedic Surgery, School of Medicine, Keio University, Tokyo, Japan
[3] Department of Applied Chemistry, School of Science and Technology, Meiji University, Kanagawa, Japan

[*] Corresponding Author E-Mail Address: n-kanza@sophia.ac.jp

Abstract: Tissue engineering has been used to enhance the utility of biomaterials for clinical bone repair by the incorporation of an osteogenic cell into a scaffold. In this study, we investigated whether apatite-fiber scaffold (AFS) can be used as a three-dimensional scaffold for cells. AFS has two different types of pores, micro and macro pores. Micro-pores, which arise from interspaces of AFS at random distribution, provide 10-μm wide spaces for cells. The other wide pores (~250-μm width), designated macro-pores; are formed after baking carbon beads, which are embedded during a preparation of AFS/beads mixed compacts. These pores formed inter-pore connections, and the pore sizes were regarded as appropriate for trapping cells. Cell-seeded scaffolds were cultured for 2 or 7 days. We evaluated the morphological changes of cultured cells such as cell attachment with optical and confocal laser scanning microscopes. These observations revealed that the seeded cells extended in Apatite-Fibers three-dimensionally, and that the cells were homogeneously distributed. These results demonstrated that seeded cells were spread equally in AFS by a simple method that involved putting some drops of cell suspension into scaffolds. Moreover, seeding efficiency was considerably higher than that of an existing commercially produced scaffold.

Introduction

Aging is one of the biggest concerns not only for Japan but also for the other countries, where the number of osteoporosis patients becomes a socially important health issue. To maintain the quality of life, autografting and allografting cancellous bone have been widely used for bone graft procedures. Moreover, synthetic grafting materials have been developed to use as a bone replacement material [1]. Hydroxyapatite (HAp) is an osteoconductive material that can be used in the bone replacement due to its chemical and crystallographic similarity to carbon-containing apatite in human bones and teeth [2]. Recently, HAp and other calcium phosphate materials are used as scaffolds that pre-embedded bone cells or other agents for the bone regeneration purposes [3]. Thus, bone tissue engineering is an emerging interdisciplinary field involving principles of the life sciences and engineering concerned with the formation of three-dimensional bone substitutes by culturing osteogenic cells on natural or synthetic scaffolds.

Our ultimate goal is to create not merely osteoconductive scaffolds, but substitutes that are able to regenerate the bones of the osteoporosis patients. In this context, we developed the apatite-fiber scaffold (AFS) as a novel scaffold for bone repair [4-6]. By changing mixture ratios of spherical carbon beads and HAp fibers, we developed scaffolds with an appropriate size of macro-pores and interconnected micro-pores. The median of the macro-pore size is ~250 μm (AFS2000), which is suitable for three-dimensional cell culture. Biological and mechanical properties of the scaffold are highly dependent on the fine structure of AFS, such as pore size, porosity, and interconnectivity [7, 8]. However, we have not yet clarified the biological effect of the AFS.

In the present study, we focused on the biological properties of the AFS; how cells are penetrated, extended and proliferated in the scaffold. Cells are expected to extend three dimensionally, similarly to the situation *in vivo*. Because cell attachment contributes to the regulation of most aspects of the cellular activity, we firstly examined the homogenous dispersion of cells into AFS. We further examined the fine structure of cells in AFS using a confocal laser scanning microscope.

Materials and Methods

Fabrication of AFS

A fibrous HAp was prepared as previously reported [4, 9]. The HAp fibers were suspended with spherical carbon beads (Nika beads; Nihon Carbon Company) with a diameter of ~150 μm in the mixed solvent (ethanol/water=1/1(v/v)) at carbon/HAp (w/w) ratio: 20/1 (AFS2000). Figure 1 shows the particular macroscopic (Fig. 1A) and scanning microscopic images (Fig. 1B) of AFS2000.

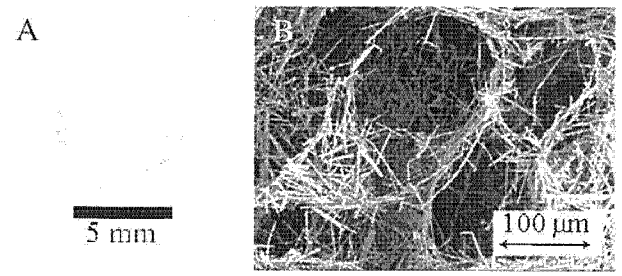

Fig. 1 Structure of AFS2000.

Pre- culture of osteoblastic cells

MC3T3-E1, osteoblastic cells were pre-cultured in a regular medium consisting of α-modified minimum essential medium (α-MEM; Sigma) supplemented with 10% heat-inactivated fetal bovine serum (FBS; Sigma) in a humidified atmosphere of 5% CO_2 at 37°C. Before the experiments, MC3T3-E1 cells were harvested by incubating with actinase and plated onto dishes at a density of 1×10^5 cells/dish (100 mm culture dish, Falcon). Culture media were changed every other day.

Cell culture in AFS

AFS was settled in each well of a 24-well culture dish (Nunclon™; Nalge Nunc Int.) and pre-wetted with 70% ethanol. An aliquot (500 μL) of cells (2.0×10^5 cells/mL) suspended in an osteogenic culture medium (regular media described above plus 20 mM β-glycerol phosphate, 4 mM L-ascorbic acid and 10 nM dexamethasone) was poured directly into each AFS. The cell-seeded AFSs were immediately filled with the osteogenic culture media. Cells were cultured in AFS in a humidified 37°C/5% CO_2 incubator for 2 or 7 days.

Preparation of freeze sections of cell-cultured AFS

MC3T3-E1 cells cultured in AFS were fixed in 4% paraformaldehyde for 15 min. Samples were washed with phosphate-buffered saline (PBS), and immersed in 1% (g/mL) gelatin/PBS solution for 60 min under reduced pressure. The specimens, embedded in O.C.T. compound (Sakura Tissue-Tek) were rapidly frozen in liquid nitrogen and stored at –20°C. Sections (18 μm) were prepared using a cryostat and placed onto Superfrost/Plus microscope slides.

Light microscopy

Sections prepared from 7 days-cultured sample were stained with hematoxylin and eosin (HE), and examined with a light microscope (Axiovert 135, Carl Zeiss Co., Ltd).

Confocal laser scanning microscopy

Sections for the confocal laser scanning microscopy (CLSM) were further incubated in 0.1% TritonX-100/PBS for 10 min, followed by washing with PBS. To visualize fibrous-actin (F-actin), we incubated samples for 30 min with Alexa Fluor 594-phalloidin (Molecular Probes Inc.) diluted 1:200 in PBS. After washing with PBS, some sections were further stained with SYTOX green (Molecular Probes Inc.) diluted 1:2000 in PBS for 10 min to visualize nuclei. The rinsed samples were mounted with antifade mounting medium and were examined by a CLSM (LSM 410, Carl Zeiss Co., Ltd.).

Three-dimensional analysis

In order to evaluate the three-dimensional cell attachment and distribution, we fixed bulks of AFS after 2-days culture with paraformaldehyde as described above. After rinsing with PBS, whole samples were stained with Alexa Fluor-phalloidin and/or SYTOX green as described above. The specimens were immersed in antifade mounting medium, and the cell-seeded surface of AFS was examined by a CLSM. Additionally, vertical torn surfaces were examined in the same way to reveal the three-dimensional cell distribution in AFS. The micrographs were processed by the adjunctive image processing software (depth coding) of CLSM.

Results

Light microscopic observation of osteoblastic cells in AFS

AFSs with 7 mm diameter and 5 mm thickness (Fig 1A) were combined with MC3T3-E1 cells by culturing for 2 or 7 days, and the frozen sections were stained with HE. Sections show that cells were mainly distributed in the same location on the fibrous structure of scaffold as indicated by arrows in Fig. 2. In addition, some macro-pores (asterisks in Fig. 2) were filled with cells, as seen in the center of the micrograph. Thus, cells were not only attached to the surface of fibrous scaffolds but also well-stretched within macro-pores. Comparison of sections at 2 or 7-days culture show that most cells were detected next to the fibrous scaffold at day 2; however, cells seemed to be tightly coupled with the fibrous structure, and the number of cells detected in macro-pores increased after 7-days incubation (data not shown).

CLSM observation with AFS sections

Immunofluorescence confocal microscopy was utilized to specify the cell distribution and to characterize the fine structure of cells in AFS (Fig. 3). Sections of AFS/cell composite cultured for 7 days were stained with the Fluor-labeled phalloidin. Phalloidin binds specifically at the interface between F-actin

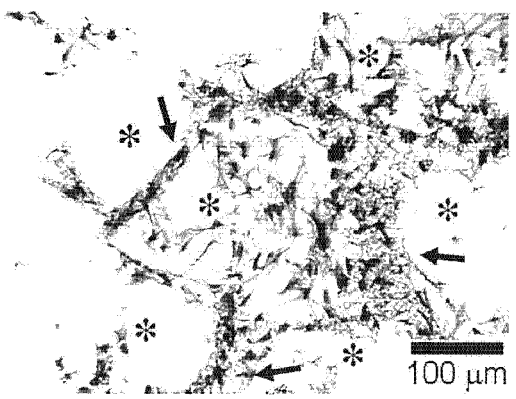

Fig. 2 HE stain image of 7-days cultured sample examined by light microscopy.

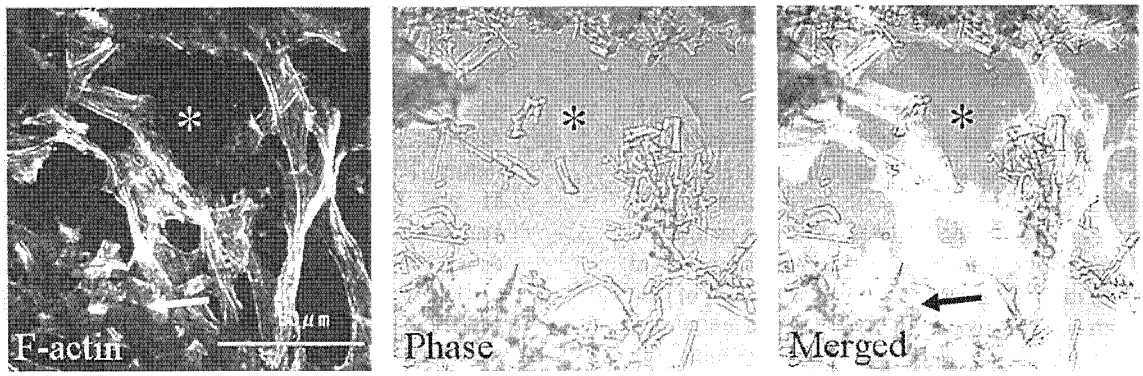

Fig. 3 Micrographs of sections examined by CLSM.

subunits; thus the cytoskeleton of each cell was specifically visualized as light-fibrous signals in a dark background (left panel in Fig. 3). Each micrograph in Fig. 3 was reorganized by assembling 20 serials of the single-plane confocal images. Merged images show that cells were distributed both near the fibrous scaffold and within a macro-pore (asterisks), which is consistent with the light microscopic observation. As shown in the left panel, cells were well stretched and microspikes extending from a single cell appeared to connect distant fibers by the tip of spikes.

The arrow in the merged image of Fig. 3 shows the pile of the HAp fibers. By light microscopy, cells were detected near the fibrous scaffold; however, fluorescence signals were detected within the pile (arrow in the left panel of Fig. 3), indicating that cells were penetrated into the micro-pores. In fact, fluorescence signals were observed within the micro-pores of the single-plane confocal image (data not shown).

CLSM observation with bulk AFS

We studied the three-dimensional distribution of cells perpendicular to the top surface of AFS. Bulks of AFS were doubly stained with Fluor-labeled phalloidin and SYTOX green, and examined by immunofluorescence confocal microscopy (Fig. 4). Each image was reassembled from 25 serials of single-plane confocal images; the total image depth was 150 μm. The nucleus of each cell can be stained with SYTOX green; thus, the localization of individual cells could be specified. CYTOX green images clearly show that cells are dispersed ubiquitously in AFS. Orientation of each cell is shown by the staining of F-actin. Fluorescence signals were mainly detected as spherical structures (asterisks) at the surfaces of macro-pores and signals were also detected within the spheres. We further analyzed images with a depth-coding program. The depth code provided the ability to show which focal planes the cells were in throughout the z-stack by assigning a color code to the pixel intensity as a function of the z-depth. The original color images show that microspikes are extended three-dimensionally, and that cells were hanging in the sphere and not merely attached to the surface (data not shown). Thus, cells were well stretched not only in micro-pores but also in macro-pores and seem to form three-dimensional cell-cell networks. Vertical cell distribution in AFS was also examined. Seeded cells were dispersed homogenously, and permeated to approximately 4-mm depth from the top surface (data not shown). These data led us to consider that three dimensional cell-cell network complexes are constructed all over the AFS.

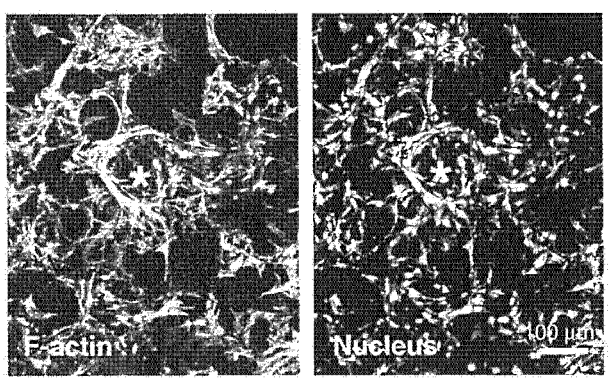

Fig. 4 Immunofluorescence micrographs of bulk AFSs by CLSM.

Discussion

Hydroxyapatite is widely applied as a biomaterial because of its biocompatibility. Several types of porous HAp ceramics have developed for the bone tissue engineering, and biochemical properties of those materials have been evaluated [1]. AFS2000 showed good cell compatibility with both osteoblastic cells and bone marrow cells and enhanced gene expression in those cells to differentiate into bone cells [5]. However, the relevance of structural feature of AFS and cell activities was not elucidated. In the present study, we clearly show that seeded cells were dispersed homogenously within AFS. By our simple seeding procedure, cells were stacked near the seeding surface of the highly porous ceramics, which is commercially available (data not shown). One of characteristic features of AFS is a high porosity, approximately 99%. Macro-pores and inter-pores function as major caviites for cell transports. In addition, micro-pores (~5 μm) composed of fibrous HAp are adequate for the circulation of culture media and nutrients, and the mesh-like structure seems to function as a trap of the appropriate number of cells. Thus, cells can permeate

all over the material through the varied cavities, resulting in the homogenous cell distribution.

Confocal laser scanning microscopy is a popular method for the soft tissue analysis; however, it still finds very limited use for the study of hard biomaterials [10]. Instead, scanning electron microscopy (SEM) is often utilized for the analysis of hard biomaterials. Although a high resolution of lateral surface images of material can be obtained by a SEM, one is unable to observe Z-axial image of the pores because of the limited depth of field of the SEM. In the present study, we utilized CLSM to evaluate the cell distribution in AFS. Additionally, to examine the fine structure of cells, we employed immunofluorescence confocal microscopy. Cells were not merely attached to the surface of scaffold but had also penetrated into micro-pores. Our novel approach showed that cells were well-stretched and extended microspikes, indicating that the size of a macro-pore is suitable for the cell growth and proliferation. Cell-cell contacts were also observed everywhere in AFS. Because cell-cell contact is essential for the cell differentiation, the complex networks may function to facilitate the gene expression of osteoblastic cells to differentiate into bone cells. Pore size and porosity are known as important parameters for osteoconduction; however, the reasons were not well explained. We considered that appropriate size of pores and high porosity provides spaces where cells can make contact with each other, resulting in the facilitated bone formation. A structural advantage of AFS is that the varied cavities composed of fibrous HAp exist everywhere in the scaffold. Thus, more complex networks of cells can be formed in AFS than in a HAp paste-based porous scaffold.

Conclusions

Apatite-fiber scaffold can provide a three-dimensional culture environment to osteoblastic cells. By our simple seeding procedure, cells were dispersed homogeneously in the scaffold. The size of macro-pores is suitable to the cell growth and proliferation. Cells were stretched within some macro-pores and penetrated into micro-pores. Structural features of AFS contributed to the formation of a cell network complex, indicating the facilitation of cell differentiation. Thus, AFS with high porosity might be a highly potent matrix for tissue engineering, leading to bone regeneration.

References

[1] Burg, K.J.L., Porter, S. and Kellam, J.F. (2000): 'Biomaterial developments for bone tissue engineering', *Biomaterials* **21**, pp. 2347-2359.

[2] Hench, L.L. (1998): 'Bioceramics', *J. Am. Ceram. Soc.*, **81**, pp. 1705-1728.

[3] Charriere, E., Lemaitre, J. and Zysset, P. (2003): 'Hydroxyapatite cement scaffolds with controlled macroporosity: fabrication protocol and mechanical properties', *Biomaterials*, **24**, pp. 809-817.

[4] Aizawa, M., Howell, F.S., Itatani, K., Yokogawa, Y., Nishizawa, K., Toriyama, M. and Kameyama, T. (2000): 'Fabrication of porous ceramics with well-controlled open pores by sintering of fibrous hydroxyapatite particles', *J. Ceram. Soc. Jpn.*, **108**, pp. 249-253.

[5] Aizawa, M., Shinoda, H., Uchida, H., Okada, I., Fujimi, T.J., Kanzawa, N., Morisue, H., Matsumoto, M. and Toyama, Y. (2004): 'In vitro biological evaluations of three-dimensional scaffold developed from single-crystal apatite fibres for tissue engineering of bone', *Phosphorus Res. Bull.*, **17**, pp. 262-268.

[6] Kawata, M., Uchida, H., Itatani, K., Okada, I., Koda, S. and Aizawa, M. (2004): 'Development of porous ceramics with well-controlled porosities and pore sizes from apatite fibers and their evaluations', *J. Mater. Sci.: Mater. Med.*, **15**, pp. 817-823.

[7] Okamoto, M., Dohi, Y., Ohgushi, H., Shimaoka, H., Ikeuchi, M., Matsushima, A., Yonemasu, K. and Hosoi, H. (2006): 'Influence of the porosity of hydroxyapatite ceramics on in vitro and in vivo bone formation by cultured rat bone marrow stromal cells', *J. Mater. Sci.: Mater. Med.*, **17**, pp. 327-336.

[8] Tsuruga, E., Takita, H., Itoh, H., Wakisaka, Y. and Kuboki, Y. (1997): 'Pore size of porous hydroxyapatite as the cell-substratum controls BMP-induced osteogenesis', *J. Biochem.*, **121**, pp. 317-324.

[9] Aizawa, M., Porter, A.E., Best, S.M. and Bonfield, W. (2005): 'Ultrastructural observation of single-crystal apatite fibres', *Biomaterials*, **26**, pp. 3427-3433.

[10] Ren, F., Smith, I.O., Baumann, M.J. and Case, E.D. (2005): 'Three-dimensional microstructural characterization of porous hydroxyapatite using confocal laser scanning microscopy', *Int. J. Appl. Ceram. Tech.*, **2**, pp. 200-211.

DEVELOPMENT OF POROUS CERAMICS WITH WELL-CONTROLLED PORE SIZES CREATED FROM SINGLE-CRYSTAL APATITE FIBERS AND ITS BIOLOGICAL EVALUATION

Y. Tanaka[1], H. Morisue[2], M. Matsumoto[2], Y. Toyama[2] and M. Aizawa[1*]

[1] School of Science and Technology, Meiji University, 1-1-1 Higashimita, Tama-ku, Kawasaki, Kanagawa, Japan 214-8571

[2] School of Medicine, Keio University, 35 Shinanomachi, Shinjyuku-ku, Tokyo, Japan 160-8582

* mamorua@isc.meiji.ac.jp

Abstract: Porous hydroxyapatite (HAp) ceramics having well-controlled porosity and pore size could be fabricated by firing apatite-fiber compacts mixed with carbon beads of 150 μm in diameter. The resulting HAp ceramics were of about 70% in porosity, and the pores were distributed in two ranges of several micrometers originating from intertwining of individual fibers and of 100-200 μm from the carbon beads. Most of the pores were regarded as open pores. The MC3T3-E1 cells cultured on/in porous HAp ceramics showed good proliferation. The cylindrical porous HAp ceramics were implanted into a tibia of rabbit, together with a control of commercially available porous HAp ceramics with porosity of 60%. After 8 weeks, newly-formed bone was abundantly present inside implants originating from the apatite fibers, as compared with the ones from the commercially available porous HAp ceramics. These results demonstrate that the present porous HAp ceramics well-controlled for the pore structure have excellent biocompatibility.

Introduction

In orthopedic surgery, bone grafting has been performed to treat diseases and injuries, such as bone tumor and bone fracture. In general, bone implantation is classified into three types: i) auto-grafting, ii) allo-grafting and iii) artificial-bone grafting. Among these bone implantations, auto-grafting is well-known as a common practice and is harvested from the patient. However, there are two serious problems as easily expected, i.e., limitations in supply from the host's bone and subsequently, the takeout surgery from the normal part of the host. Alternatively, allo-grafting has been performed using donor bones obtained from bone banks; however, it also has problems of supply, immunogenic factors and quality. Thus, for artificial-bone grafting, which would have the least problem in the implantation, porous HAp ceramics, which can be integrated with newly-formed bone of the host, are generally used [1].

Porous HAp ceramics for bone-grafting are required to contain interconnected open pores whose sizes of over 100 μm in diameter [2], to lead to penetration and proliferation of osteoblasts, vascular ingrowths and integration of newly-formed bone into porous ceramics. Microstructure of porous ceramics with interconnected open pore is also effective for being saturated with a body fluid or as mediums for cell culture.

Previously, porous HAp ceramics have been fabricated via the following processes [1,3,4]: i) sintering of the HAp particle in the co-presence of naphthalene particles or hydrogen peroxide, ii) utilization of apatite cement prepared from tetracalcium phosphate ($Ca_4O(PO_4)_2$) and calcium hydrogen phosphate ($CaHPO_4$), and iii) HAp conversion by hydrothermal reaction of marine invertebrates with diammonium hydrogen phosphate ($(NH_4)_2HPO_4$).

Using single-crystal apatite fibers [5], we have developed the porous HAp ceramics with well-controlled porosity and interconnected open pores [6]. In addition, we have successfully prepared the porous HAp ceramics with pores of over 100 μm in diameter by firing the apatite-fiber compacts mixed with carbon beads [7].

Our aims of the present investigation were to fabricate porous HAp ceramics from apatite fiber and carbon beads, and then to examine *in vitro/vivo* the biocompatibilities of the resulting porous ceramics.

Materials and Methods

Fabrication of porous ceramics and their characterization

As previously reported [5], single-crystal apatite fibers were synthesized by a homogeneous precipitation method from $Ca(NO_3)_2$-$(NH_4)_2HPO_4$-$(NH_2)_2CO$-HNO_3-H_2O solution. The starting solution having a Ca/P ratio of 1.67 was prepared by mixing 0.167 mol· dm^{-3} $Ca(NO_3)_2$, 0.100 mol· dm^{-3} $(NH_4)_2HPO_4$, 0.500 mol· dm^{-3} $(NH_2)_2CO$ and 0.10 mol· dm^{-3} HNO_3 aqueous solutions. The solution was heated at 80 °C for 24 h and then at 90 °C for 72 h to synthesize apatite fibers.

Porous HAp ceramics were fabricated from the apatite fibers as follows [7]: the fibers were suspended into pure water to prepare the slurry with apatite contents of 2 mass%. Carbon beads with 20 or 150 μm in average diameter (Nikabeads; Nihon Carbon

Company, Japan) were added to the apatite-fiber slurry in the carbon/HAp ratio of 1/1(w/w). Then, an agar was added to the carbon/HAp mixed slurry so as to be at 0.10 mass%. The resulting slurry was heated using a hot plate to dissolve the agar, and then ethanol was added to the slurry at a ratio of 7/3(v/v) for water/ethanol. After stirring the slurry, it was allowed to cool to room temperature. This slurry was poured into vinyl chloride tubes of 17 mm in inner diameter and suction-filtrated to prepare the precursors of green compacts. After the precursors were air-dried at room temperature, they were uniaxially compressed at 40 MPa to form the green compacts. The porous HAp ceramics were fabricated by firing the green compacts at 1300 °C for 5 h in steam atmosphere. Hereafter, the porous HAp ceramics using carbon beads of 20 and 150 μm in average diameter are hereafter named "P-HAp(20)" and "P-HAp(150)", respectively; the porous HAp ceramics fabricated by firing the carbon-free apatite-fiber compacts uniaxially compressed at 30 MPa were named "P-HAp(0)".

The crystal phases of the P-HAp(0), (20) and (150) were identified by X-ray diffractometry (XRD) and Fourier-transform infrared spectroscopy (FT-IR), and the microstructures were observed by scanning electron microscopy (SEM).

The relative density of the porous ceramics was calculated by diving the bulk density by the theoretical density (3.16 $g \cdot cm^{-3}$) of HAp. The total porosity was estimated by subtracting the relative density from 100%. The open and closed porosities were determined on the basis of the apparent density of the porous ceramics measured by picnomerty.

In vitro evaluation using osteoblast model

The resulting porous HAp ceramics were biologically evaluated using the osteoblastic cell, MC3T3-E1 [8]. About 5.0×10^4 cells were seeded on the P-HAp(0), P-HAp(20), P-HAp(150), dense HAp ceramics and control (24-well plate for cell culture) after soaking these specimens in α-minimum essential medium supplied with fetal bovine serum (α-MEM(+)) for 24 h. Dense HAp ceramics were fabricated from commercially available HAp powder (HAp-100; Taihei-kagaku company, Japan). We examined the proliferation and morphology of the cells cultured for 1, 3, 5 and 7 days on/in the above-mentioned specimens. As for the cell proliferation, we performed a WST-1 assay using a kit of Premix WST-1 Cell Proliferation Assay System (TAKARA BIO INC, Japan). Cell morphology was observed by a SEM after fixation and freeze-drying.

In vivo evaluation using rabbit model

We performed a biocompatibility test using rabbit (Japan white, 16 weeks old, male, weight ~ 3 kg) model. The specimens used *in vivo* evaluation were P-HAp(150) and APACERAM [9] (control; PENTAX Corporation, Japan). Cylindrical P-HAp(150) with porosity of 70% and APACERAM with porosity of 60% (the size of 4.0 mm in diameter, ~ 8 mm in height) were implanted into tibiae of rabbits. At 8 weeks after implantation, the rabbits were sacrificed to retrieve the specimens with the surrounding bone tissue, and then undecalcified sections were prepared for the histological evaluation. The sections were stained with hematoxylin and eosin (HE) stain.

Results and discussion

Characterization of porous HAp ceramics for biological testing

Figure 1 shows the XRD patterns of a series of the P-HAp(0), (20) and (150). The pure HAp phase was present in the P-HAps. The absorptions of the P-HAps in the FT-IR spectra were assigned to typical HAp.

Figure 2 shows total, closed and open porosities of P-HAps. Total porosities of P-HAp(0), (20) and (150) were about 40%, 70% and 70%, respectively. Most of the pores in the P-HAps could be regarded as open pores. This result indicates that the resulting ceramics contain open pores which develop the continuous three-dimensional structure inside the ceramics.

Figure 3 illustrates the microstructures of the P-HAps. The carbon-free P-HAp(0) contains pores with the sizes of several micrometers originating from intertwining of individual fibers. Meanwhile, the P-HAp(20) and P-HAp(150) posess two kinds of pores with the sizes of several micrometers derived from intertwining of individual fibers and of about 20 μm or 100-200 μm from the carbon beads. Ioku et al. have reported that the porous ceramics with bimodal pore-size distribution have enhanced bioresorbability and biocompatibility [10]. We have concluded that the present P-HAp(150) having both an interconnected open pore and pores of over 100 μm in diameter will be especially effective for the osteointegration with newly-formed bone of the host.

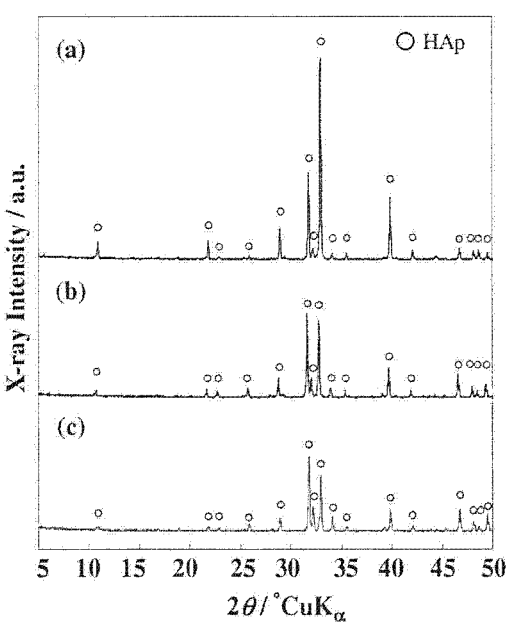

Fig.1 XRD patterns of the P-HAps:
(a) P-HAp(0), (b) P-HAp(20) and (c) P-HAp(150).

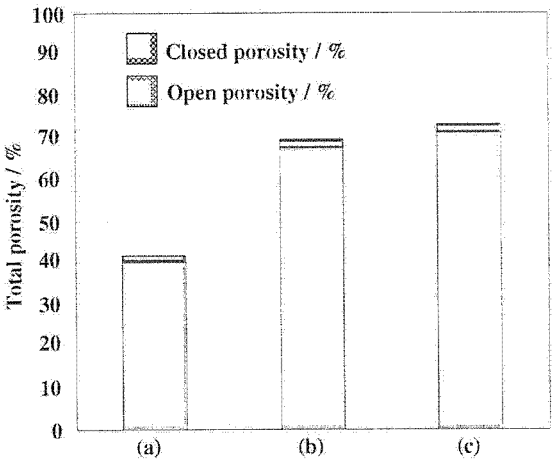

Fig. 2 Total, closed and open porosies of (a) P-HAp(0), (b) P-HAp(20) and (c) P-HAp(150).

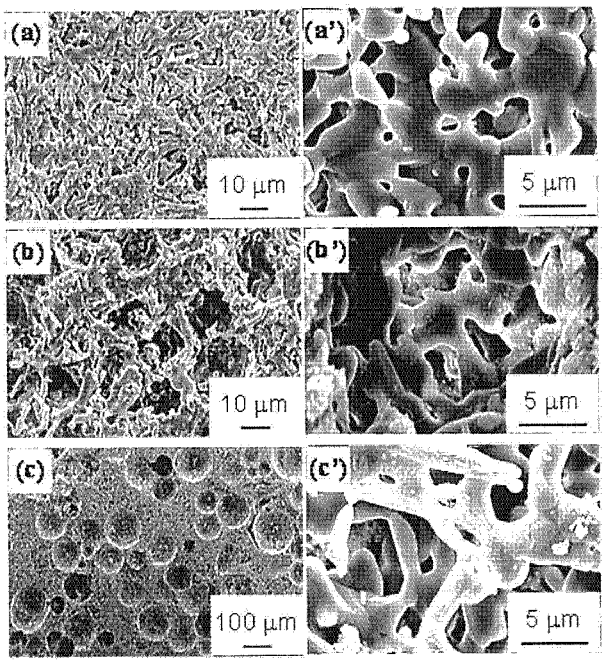

Fig. 3 SEM images of (a)(a') P-HAp(0), (b)(b') P-HAp(20) and (c)(c') P-HAp(150).

Proliferation of MC3T3-E1 on the P-HAps

For cell toxicity test, we examined proliferation of cells seeded on the P-HAps, dense HAp ceramics (positive control) and control (polystyrene cell-culture 24-well plate). The results of WST-1 assay are shown in Fig. 4. The MC3T3-E1 cells cultured on all the specimens showed good proliferation.

Figure 5 shows the morphologies of the MC3T3-E1 cells cultured on the P-HAp(150) for 3 and 7 days. Morphological observation indicated that the MC3T3-E1 cells attached on the surface and inside macro-pores (100-200 μm in diameter) of the ceramics to proliferate up to nearly confluent. Meanwhile, in the cases of the P-HAp(0) and P-HAp(20) having pores of less than 100 μm in diameter, the MC3T3-E1 cells proliferated only

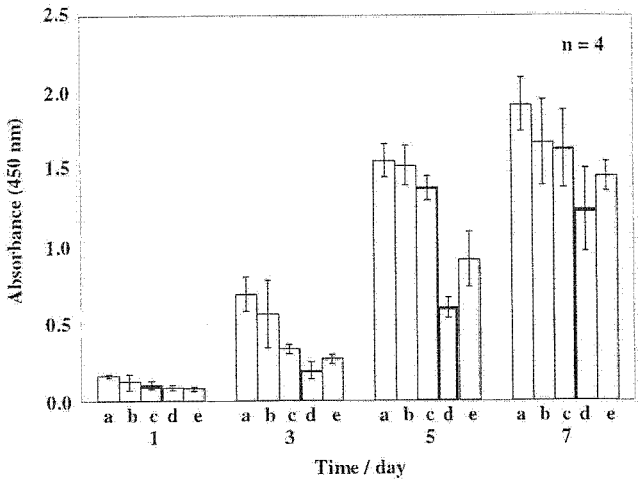

Fig. 4 Proliferation of the MC3T3-E1 cells on/in (a) Control, (b) Dense HAp ceramics, (c) P-HAp(0), (d) P-HAp(20) and (e) P-HAp(150).

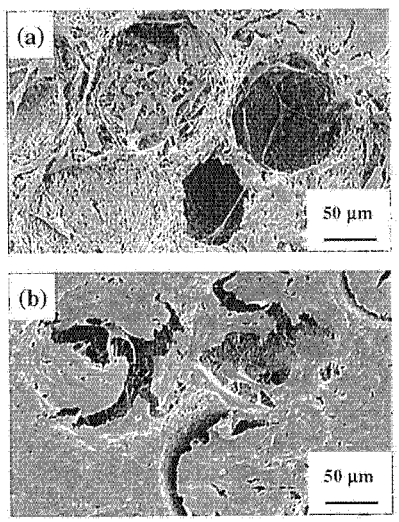

Fig. 5 Morphology of the MC3T3-E1 cells cultured on/in the P-HAp(150) for (a) 3 days and (b) 7 days.

on the surface of the ceramics. These results indicated that all the P-HAps had no cell-toxicity, and especially, the P-HAp(150) may promise the osteointegration with newly-formed bone of the host.

Histological evaluation

At 8 weeks after implantation, we performed histological evaluation with HE stain using sections of tibiae containing the implanted P-HAp(150) and a control. The results of the histological observation are shown in Fig. 6. Osteoblasts were present in both P-HAp(150) and control, and vascular formation was also observed in the central area of the porous ceramics. The P-HAp(150) showed excellent osteoconductivity, as compared with a control. These results indicated that the P-HAp(150) induced an excellent osteointegration with living hard tissues of the host. This may be due to the specific pore structure of the P-HAp(150) originating from single-crystal apatite fibers.

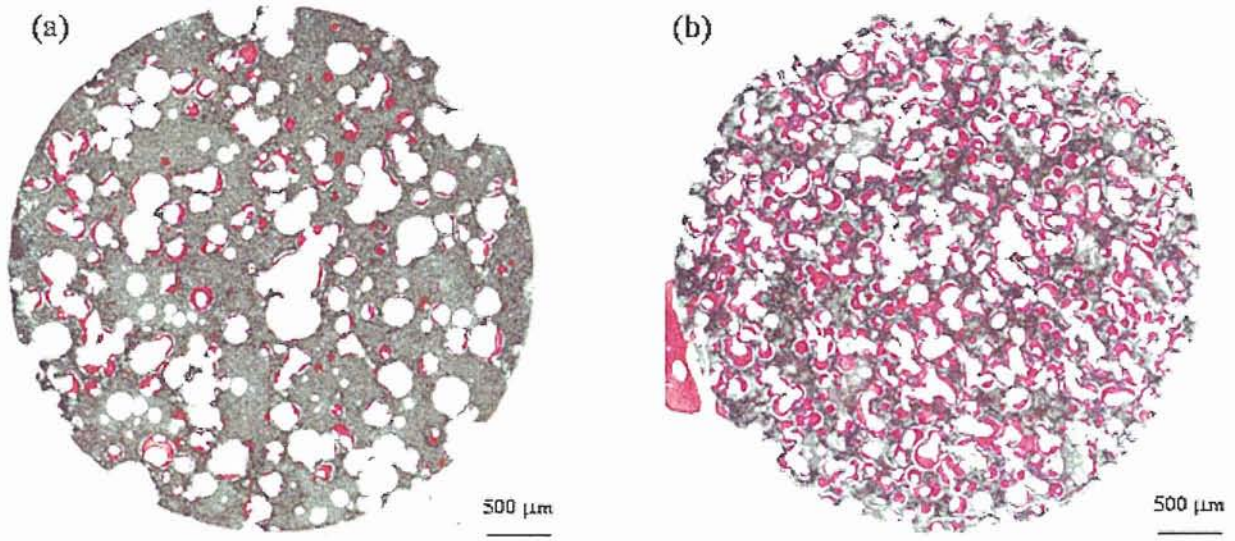

Fig. 6 Histological evaluation with HE stain of
(a) Control (APACERAM) and (b) P-HAp(150) at 8 weeks after implantation.

Conclusion

We have successfully fabricated porous HAp ceramics with well-controlled pore sizes using both single-crystal apatite-fibers and carbon beads with 150 μm in diameter, and then examined the biocompatibility of the resulting ceramics *in vitro*/*vivo*. The examination of cell growth showed that the MC3T3-E1 cells cultured on/in porous HAp ceramics have good proliferation. At 8 weeks after implantation, the histological evaluation showed excellent osteoconductivity, as compared with a control. We conclude that the present P-HAp(150) may be a high-performance artificial bone graft, which will leads enhance the osteointegration with newly-formed bone of the host.

Acknowledgment

A part of the present research has been defrayed by ''Academic Frontier'' Project for Private Universities: matching fund subsidy from MEXT (Ministry if Education, Culture, Sports, Science and Technology), 2006 ~ 2010.

References

[1] R. Z. LeGeros and J. P. LeGeros (1993):'Dense hydroxyapatite', in L. L. Hench and J. Wilson (Ed):'An introduction to bioceramics' (World Scientifi), pp. 139-80

[2] N. Tamai, A. Myoui, T. Tomita, T. Nakase, J. Tanaka, T. Ochi and H. Yoshikawa (2001): 'Novel hydroxyapatite ceramics with an interconnective porous structure exhibit superior osteoconduction *in vivo*', *J. Biomed. Mater. Res.*, **59**, pp. 110-117

[3] C. Klein, P. Patka and W. den Hollander (1989): 'Macroporous calcium phosphate bioceramics in dog femora: a histological study of interface and biodegration', *Biomaterials*, **10**, pp. 59-62

[4] D. M. Roy and S. K. Linnehan (1974): 'Hydroxyapatite formed from coral skeletal carbonate by hydrothermal Exchange', *Nature*, **247**, pp. 220-22

[5] M. Aizawa, A. E. Porter, S. M. Best and W. Bonfield (2005): 'Ultrastructural observation of single-crystal apatite fibres', *Biomaterials*, **26**, pp. 3427-3433

[6] M. Aizawa, F. S. Howell, K. Itatani, Y. Yokogawa, K. Nishizawa, M. Toriyama and T. Kameyama (2000) : 'Fabrication of porous ceramics with well-controlled open pores by sintering of fibrous hydroxyapatite particles', *J. Ceram. Soc. Jpn.*, **108**, pp. 249-253

[7] M. Kawata, H. Uchida, K. Itatani, I. Okada, S. Koda and M. Aizawa (2004): 'Development of porous ceramics with well-controlled porosities and pore sizes from apatite fibers and their evaluations', *J. Mater. Sci.: Mater: Med.* , **15**, pp. 817-823

[8] H. Sudo, H. Kodama, Y. Amagai, S. Yamamoto and S. Kasai (1983): '*In Vitro* differentiation and calcification in a new clonal osteogenic cell line derived from newborn mouse calvaria', *J. Cell Biol.*, **96**, p. 191

[9] T. Ogawa, K. Abe, Y. Tominaga and T. Nakajima (2003): 'Material design and clinical applications of hydroxyapatite ceramic bone grafts', *Bull. Ceram. Soc. Jpn.*, **38**, pp. 51-54

[10] H. Yokozeki, T. Hayashi, T. Nakagawa, H. Kurosawa, K. Shibuya and K. Ioku (1998): 'Influence of surface microstructure on the reaction of the active ceramics *in Vivo*', *J. Materi. Sci.: Mater. Med.*, **9**, pp. 381-384

THREE-DIMENSIONAL CELL CULTURE OF HEPATOCYTES USING APATITE-FIBER SCAFFOLD AND APPLICATION TO A RADIAL-FLOW BIOREACTOR

A. Hiramoto[1], T. Matsuura[2] and M. Aizawa[1,*]

[1]Department of Applied Chemistry, School of Science and Technology, Meiji University,1-1-1 Higashimita, Tama-ku, Kawasaki, Kanagawa, Japan 214-8571

[2]Division of Central Clinical Laboratory, Jikei University Hospital, 3-19-18 Nishi-shinbashi, Minato-ku, Tokyo, Japan 105-8461

*mamorua@isc. meiji. ac. jp

Abstract: We have successfully developed apatite-fiber scaffolds (AFSs) for bone tissue engineering using the single-crystal apatite fibers and carbon beads. In the present investigation, we examined the possibility of three-dimensional (3D) culture of hepatocytes using the AFSs, aiming to apply the scaffold as a matrix of the artificial liver model. FLC-4 cells were used as a model of hepatocyte. The results of cell proliferation showed that the FLC-4 cells 3D-cultured in the AFS have higher DNA contents than that on cell-culture polystyrene plate for control. The morphological observation showed that the FLC-4 cells adhered thoroughly to AFS. In order to assay the function as a hepatocyte, we determined the amount of albumin produced from FLC-4 cells during cell culture periods by an ELISA method; the albumin in the medium was used for assay. The amount of albumin production increased with cultivation time. In another experiment using a radial-flow bioreactor (RFB), the FLC-4 cells were viable in the RFB over a period for 21 days. The amounts of glucose and lactic acid were measured during 3D-cell culture using the RFB. The amounts of glucose decrease, while that of lactic acid increased. These changes indicate that the FLC-4 cells were fully grown in the RFB.

Introduction

Recently, a liver transplant increases year by year; however, it has a fatal problem of donor's lack. Thus, the development of the artificial liver that assists the liver function is being needed. Tissue engineering is noticed as one of the solutions to the above problem, and it regenerates the defected lacked tissue by combining three factors: cells, growth factors and scaffold.

We have succeeded in development of the scaffold with interconnected macro-pores, which enable three-dimensional cell culture, using single-crystal apatite fibers (AFs) and carbon beads [1, 2]. This scaffold is named as "apatite-fiber scaffold (AFS)". The AFS has an excellent biocompatibility to osteoblast *in vitro* and hard tissues *in vivo*.

In order to apply the above AFS to the regeneration of real organs (for example, liver), we performed the culture of FLC-4 cells [3] as a model of hepatocyte. Furthermore, we examined the proliferation and morphology of the hepatocytes in the AFS.

As for the evaluation of function as a hepatocyte, we determined the amount of albumin which one of the vital proteins produced from FLC-4 cells.

In order to realize three-dimensional cell culture, we used a radial-flow bioreactor (RFB). A RFB enables a highly functional three-dimensional culture as bio-artificial liver [4]. The capacity of bioreactors depends not only on their mechanistic structures but also on scaffolds packed in them. Thus, we carried out three dimensional (3D) cell culuture using the RFB settled with AFS over periods for 21 days, and assessed the viability of FLC-4 cells by monitoring pH, concentrations of glucose and lactic acid. Instead of the AFSs, cellulose beads were also settled into the RFB as a control in the present work.

Materials and Methods

Materials

The AF was synthesized via a homogeneous precipitation method using urea [5, 6]. The AF was mixed with the spherical carbon beads having a diameter of ~150 μm in the mixed solvent (ethanol/water=5/5(v/v)). As previously reported in Ref [1,2], the carbon beads were added to the AF in the following carbon/HAp (w/w) ratios: 20/1, 10/1 and 0/1. The resulting compacts were fired at 1300 °C for 5 h in a steam atmosphere to fabricate the AFS; hereafter, we named each scaffold derived from carbon/HAp=20/1, 10/1 and 0/1 (w/w) as "AFS2000", "AFS1000" and "AFS0", respectively.

The crystal phase of the AFS was identified with an X-ray diffractometer (XRD) and a Fourier transform infrared spectrometer (FT-IR), and the microstructure was observed by a scanning electron microscope (SEM).

Cells culture

The resulting scaffolds were biologically evaluated using the FLC-4 cells. The cell is derived from human hepatocellular carcinoma, which is one of the cell-line of hepatocyte established by Matsuura [3]. Table 1 gives some properties of the current cell; the morphology is also shown in Fig. 1. As this cell well-maintains the function of hepatocyte, such as albumin production, it can be used as a model cell-line for development of artificial liver organ.

Table 1 properties of the FLC-4 cell [3].

Histogen	hepatocarcinoma
HBV antigen production [EIA]	-
HCV [RT-PCR]	-
Doubling time	40 h
Albumin production [EIA]	18 μg/10^5 cells/day
AFP production [EIA]	0.007 μg/10^5 cells/day
Detoxification capacity (ammonia)	+

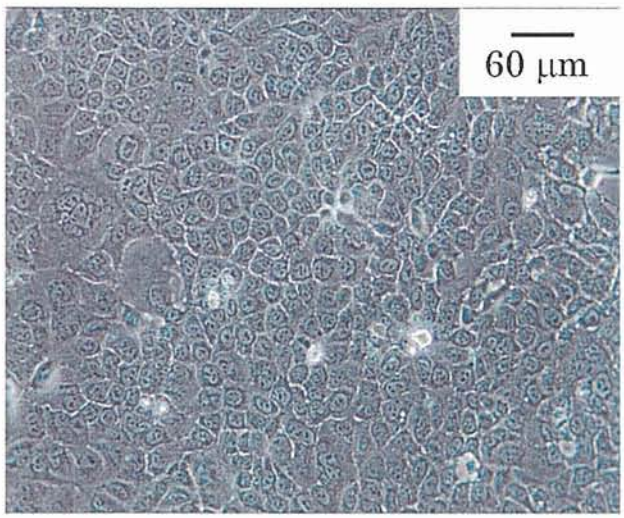

Fig. 1 Morphology of the FLC-4 cells (7 days).

The FLC-4 cells were grown in AFS104 (Ajinomoto, Japan) of serum-free culture medium without the unknown proteins. The cells of 5.0×10^5 were seeded on the AFS2000 (sample size: 7.5 mmϕ in a diameter × 3.5 mm in height), AFS1000 (7.5 mmϕ× 2.5 mm), AFS0 (7.5 mmϕ× 1 mm) and control (polystyrene; 48-well plate for cell culture). We examined the proliferation and morphology of cells cultured for 1 to 21 days. As for the cell proliferation, we measured the DNA content produced from cells by fluorometry using the Hoechst 33258 agent. Cell morphology was observed by a SEM after fixation and followed freeze-drying.

Determination of albumin produced from cells

The amount of albumin produced into the medium was quantified using a human albumin ELISA quantitation kit (Bethyl Laboratories) under the conditions recommended by the manufacturer. A calibration curve was drawn using purified human albumin (Bethyl Laboratories).

Three-dimensional culture using a radial-flow bioreactor

A radial-flow bioreactor system (Able Co.) with a chamber volume of 5 cm^3 was used for three-dimensional cell culture of FLC-4 cells. AFS2000 with the sizes of 17 mm in a diameter and 14 mm in a thickness was setteled into the bioreactor, as illustrated in Figure 2. Instead of AFS2000, granular-shaped cellulose beads with sizes of 1 mm were also used as a control.

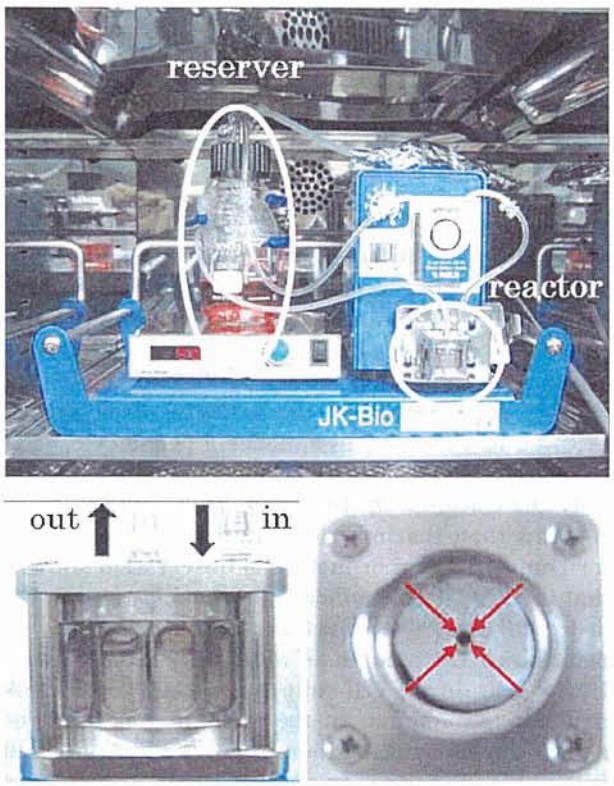

Fig. 2 Overview of radial-flow bioreactor system.

As for seeding of the FLC-4 cells into scaffolds, cells of 3.0×10^6 were added to the medium reserver, and then the medium was circulated at 2.5 $cm^3 \cdot min^{-1}$. The medium was exchanged the flesh one every 7 days. In order to assess a viability of FLC-4 cells, the concentrations of glucose and lactic acid in the medium were monitored during a circulating cell culture up to 21 days, together with pH measurement.

Results and discussion

AFS, a porous scaffold

Figure 3 shows the XRD patterns of a series of AFS. The single HAp phase was present in the AFS0, AFS1000 and AFS2000. The FT-IR spectra showed that the absorptions of the AFSs were assigned to typical HAp.

Figure 4 illustrates the microstructures of the AFSs. AFS1000 and AFS2000 had a large pore sizes and high porosity (98% or higher), compared with those of the carbon-free AFS0 scaffold. The median pore size was

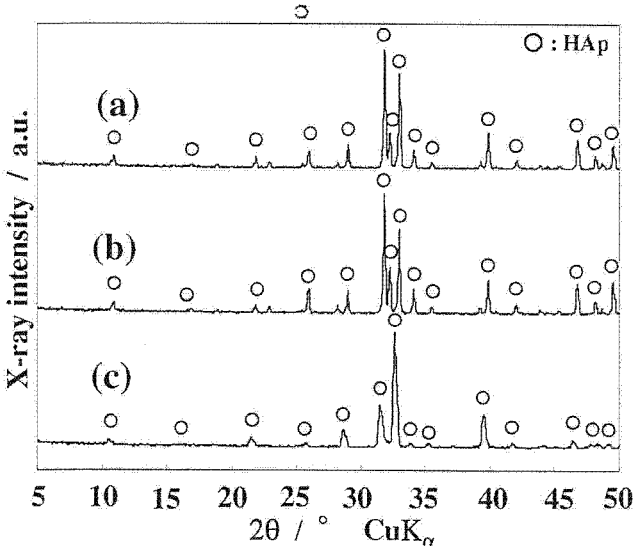

Fig. 3 XRD patterns of (a) AFS2000, (b) AFS1000 and (c) AFS0.

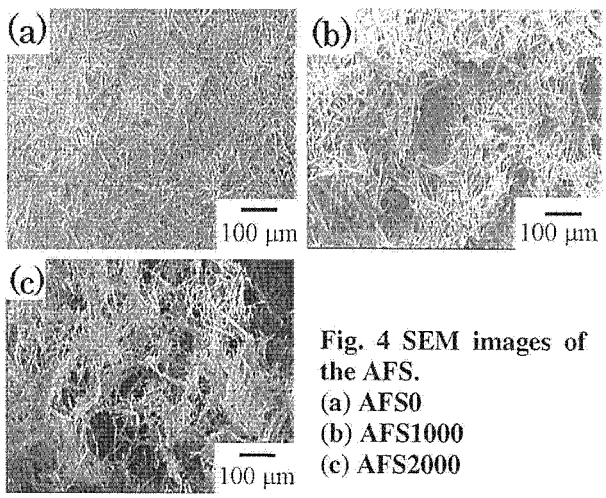

Fig. 4 SEM images of the AFS.
(a) AFS0
(b) AFS1000
(c) AFS2000

~5 μm in AFS0, ~110 μm in AFS1000, and ~250 μm in AFS2000. We concluded that the AFS2000, especially, possessed a pore size suitable for the cells to easily enter into the scaffold.

Proliferation of FLC-4 cells in AFS

Using the above-mentioned AFSs, we examined proliferation of cells seeded in the AFSs. The results were shown in Figure 5. Although the cells were well-proliferated in/on all the specimens examined, the cells in the AFS group were much grown than that on the control. Especially, the cells in AFS2000 proliferated in a similar manner to those on the AFS0 and AFS1000 from 1 d up to 7 d and more efficiently after that to 21 d. This result of good cell proliferation may be due to the 3D structure of the AFS2000.

Figure 6 shows the morphologies of the FLC-4 cells cultured in the AFS0 and AFS2000 for 7 days. In the case of AFS2000, the cells were three-dimensionally attached in the macro-pores to grow up to nearly confluent. The SEM observation revealed that the AFS2000 scaffold was able to support 3D cell proliferation compared with AFS0.

It could be seen from *in vitro* evaluation using a cell-line of hepatocyte that the above-mentioned scaffolds

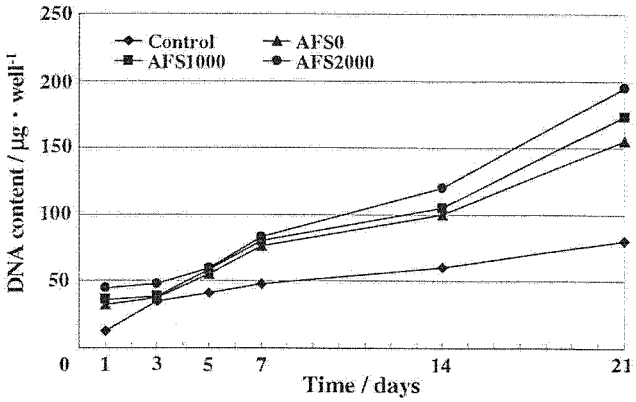

Fig. 5 Growth curves of the FLC-4 cells in AFSs, together with control.

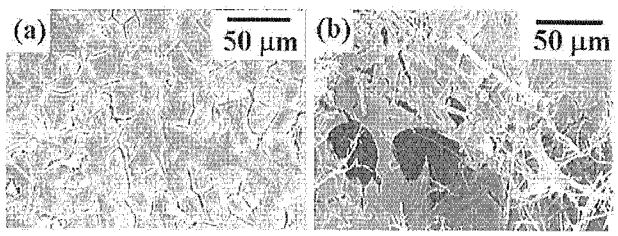

Fig. 6 Morphology of the FLC-4 cells cultured in (a) AFS0 and (b) AFS2000 for 7 days.

had an excellent cellular response, including good initial cell-attachment efficiency (1 day) and subsequent proliferation (3 to 21 days).

Albumin production

As a marker of cell function of hepatocyte, we determined the amount of albumin secreted into the culture medium by ELISA. Figure 7 shows the amount of albumin secreted into the medium in AFS2000 over a cultivation period for 7 days.

In the 1 day, the amount of albumin produced in AFS1000 and AFS2000 was remarkably lower than that of control. This difference may be due to the adsorption of albumin to AFS consisting of apatite fibers with preferred orientation to *a*-plane. The *a*-plane of HAp crystal is positively charged to well-adsorb acidic proteins (albumin) with negative charge.

The amount of albumin secreted from FLC-4 cells

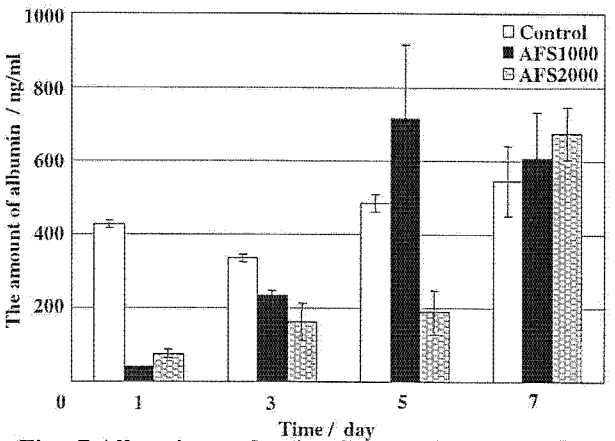

Fig. 7 Albumin production from cells cultured in AFS2000 over a period of 7 days.

cultivated in AFS2000 gradually increased over a period of 7 days. In the 7 days, the amount of albumin produced from FLC-4 cells in the 3-D culture using AFSs was greater than that produced in the 2-D culture using control.

Monitoring the viability of FLC-4 cells in the RFB

Next, the FLC-4 cells were three-dimensionally cultured using a RFB. In general, cells spend glucose to produce a lactic acid via metabolism. Thus, we monitored the concentrations of glucose and lactic acid in the medium over a period of 21 days. The results of AFS2000 are shown in Fig. 8, together with that of cellulose beads.

The concentration of the glucose decreased with culture time, while that of the lactic acid increased. This decrease of the glucose concentrations corresponds to the increase of the lactic acid. The glucose concentration were recovered once the medium were exchanged with fresh one every 1 week. The glucose concentration decreased instead of increase of the lactic acid again. In addition, the pH in the medium slightly decreased with increase of the lactic acid. We monitored the concentrations of glucose and lactic acid to confirm the vigorous growth of the FLC-4 up to 21 days clear. As compared with cellulose beads, the AFS2000 showed good cell prolification.

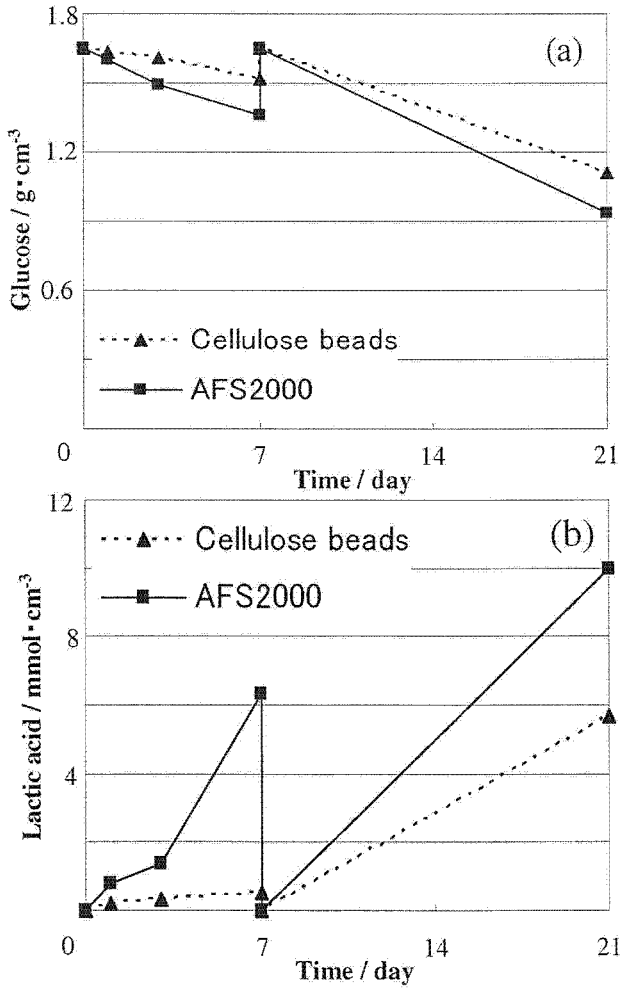

Fig. 8 Changes of (a) glucose and (b) lactic acid in ASF104 medium in the RFB over a period of 21 days.

Conclusions

In order to apply the AFS as a matrix of the artificial liver, we performed the three-dimensional cell culture using the AFS and FLC-4 cells as a model of hepatocyte. The results of cell proliferation showed that the FLC-4 cells cultured in the AFS have higher DNA contents than that on polystyrene plate for cell culture. Among the AFSs examined, the AFS2000 indicated the best cell proliferation. The amount of albumin produced from FLC-4 cells in the 3-D culture using AFSs was greater than that produced in the 2-D culture using control.

In another experimental using a radial-flow bioreactor (RFB), the FLC-4 cells were well-viable in the RFB settled with AFS2000 over a period for 21 days, compared with the case of cellulose beads. We conclude that the present AFS may be a promising scaffold for tissue engineering of liver.

References

[1] Aizawa, M., Shinoda, H., Uchida, H., Okada, I., Fujimi, T. J., Kanzawa, N., Morisue, H., Matsumoto, M. and Toyama, Y. (2004): 'In vitro biological evaluations of three-dimensional scaffold developed from single-crystal apatite fibres for tissue engineering of bone', *Phos. Res. Bull.*, **17**, pp. 262-268.

[2] Aizawa, M., Shinoda, H., Uchida, H., Itatani K., Okada, I., Matsumoto, M., Morisue, H.,Matsumoto, H. and Toyama, Y. (2003): 'Development and Biological Evaluation of Apatite Fiber Scaffolds with Large Pore Size and High Porosity for Bone Regeneration', *Key Engineer. Mater.*, **240-242**, pp. 647-650.

[3] Matsuura, T. (1997): 'Cell sources for bioartificial liver - Hepatocytes and smusoidal cells -', *Tissue culture engineering*, **23**, pp. 288-291.

[4] Iwahori, T., Matsuura, T., Maehashi, H., Sugo, K., Saito, M., Hosokawa, M., Chiba, K., Masaki, T., Aizaki, H., Ohkawa, K. and Suzuki, T. (2003): 'CYP3A4 inducible model for in vitro analysis of human drug metabolism using a bioartificial liver', HEPATOLOGY, **37**, pp. 665-673.

[5] Aizawa, M., Howell, F. S., Itatani, K., Yokogawa, Y., Nishizawa, K., Toriyama, M. and Kameyama, T. (2000): 'Fabrication of porous ceramics with well-controlled open pores by sintering of fibrous hydroxyapatite particles', *J. Ceram. Soc. Jpn.*, **108**, pp. 249-253.

[6] Aizawa, M., Porter, A. E., Best, S. M. and Bonfield, W. (2005): 'Ultrastructural observation of single-crystal apatite fibres', *Biomaterials*, **26**, pp. 3427-3433.

Polymerizable Cationic Gemini Surfactant

Masahiko Abe,[†,‡] Kazuyuki Tsubone,*[,†] Takaaki Koike,[†] Koji Tsuchiya,[‡] Takahiro Ohkubo,[‡] and Hideki Sakai[†,‡]

Faculty of Science and Technology, Tokyo University of Science, 2641 Yamazaki, Noda, Chiba 278-8510, Japan, and Institute of Colloid and Interface Science, Tokyo University of Science, 1-3 Kagurazaka, Shinjuku, Tokyo 162-8601, Japan

Received January 17, 2006. In Final Form: June 1, 2006

A polymerizable cationic gemini surfactant, $[CH_2{=}C(CH_3)COO(CH_2)_{11}N^+CH_3)_2CH_2]_2{\cdot}2Br^-$, **1** has been synthesized and its basic interfacial properties were investigated (in water and in the presence of 0.05 M NaBr). For comparison, the properties of monomeric surfactant corresponding to **1**, $CH_2{=}C(CH_3)COO(CH_2)_{11}N^+(CH_3)_3{\cdot}Br^-$, **2**, were also investigated. Parameters studied include cmc (critical micelle concentration), C_{20} (required to reduce the surface tension of the solvent by 20 mN/m), γ_{cmc} (the surface tension at the cmc), Γ_{cmc} (the maximum surface excess concentration at the air/water interface), A_{min} (the minimum area per surfacatant molecule at the air/water interface), and cmc/C_{20} ratio (a measure of the tendency to form micelles relative to adsorb at the air/water interface). For the polymerizable gemini surfactant, **1**, the methacryloxy groups at the terminal of each hydrophobic group in a molecule have no contact with the air/water interface in the monolayer, whereas for the corresponding monomeric surfactant, **2**, the methacryloxy group contacts at the interface forming a looped configuration like a bolaamphiphile. Polymerized micelles of the gemini surfactant are fairly small monodisperse and spherical particles with a mean diameter of 3 nm.

In the past decade, new types of surfactant called gemini surfactants (or sometimes called dimeric surfactants) having two hydrophobic tails and two hydrophilic headgroups connected through a linkage adjacent to the hydrophilic headgroups in a molecule have attracted considerable interest since these compounds have very much lower cmc values and much greater efficiency in reducing surface tension (pC_{20}) than expected.[1a] These properties result from the fact that the hydrophobic groups of gemini surfactant molecules can pack at the interface more closely than those of the corresponding monomeric surfactants, especially when the linkage consists of two methylene groups.[1a] Owing to their extraordinary surface activity, they are regarded as an outstanding new generation of surfactants with excellent solubilization, wetting, and rheological properties at low concentration.[2]

On the other hand, polymerizable surfactants have been used in a variety of application including capturing the structure of spherical micelles[3,4] and as a stabilizer in emulsion polymerization,[5,6] miniemulsion polymerization,[7] and microemulsion polymerization.[8] Kaler et al. showed that polymerizable anionic wormlike micelles were obtained upon mixing the hydrotropic salt *p*-toluidine hydrochloride with the polymerizable anionic surfactant sodium 4-(8-methacryloyloxyoctyl)oxybenzene sulfonate.[9] Polymerization captures the cross-sectional radius of the micelles (~2 nm), induces micellar growth, and leads to the formation of a stable single-phase dispersion of wormlike micelles polymers. Walker et al. synthesized a cationic surfactant of the form (C_nH_{2n+1}) trimethylammonium 4-vinylbenzoate (where n = 14−18) and investigated the parameters necessary to independently control the final radius and length of rodlike polymerized aggregates.[8] Sodium di(undecenyl)tartarate,[10] one of the polymerizable gemini surfactant, has recently been investigated as novel pseudostationary phases in micellar electrokinetic chromatography.[11] The lyotropic liquid-crystalline phase bahavior of cross-linkable and polymerizable gemini surfactants, bis(alkyl-1,3-diene)-based phosphonium amphiphiles, has been studied to design nanostructures.[12] Very little information is found in the literature on polymerizable gemini surfactants with the exception of these two species. We report in this paper the interfacial properties of a novel polymerizable cationic gemini surfactant with a polymerizable group at the terminal of each hydrophobic group, $[CH_2{=}C(CH_3)COO(CH_2)_{11}N^+(CH_3)_2CH_2]_2{\cdot}2Br^-$, **1**, while comparing with those of the monomeric surfactant corresponding to the gemini **1**, $CH_2{=}C(CH_3)COO(CH_2)_{11}N^+(CH_3)_3{\cdot}Br^-$, **2**,[13] conventional cationic surfactants, tetradecyltrimethylammonium bromide (TTAB), and cetyltrimethylammonium bromide (CTAB). The interfacial properies of studied include cmc, pC_{20} (negative logarithmic molar surfactant concentration required to reduce the surface tension of the solvent by 20 mN/m), γ_{cmc} (surface tension value at cmc), Γ_{max} (maximum surface excess concentration at air/water interface), A_{min} (minimum area occupied by one surfactant molecule at air/water interface), and cmc/C_{20} ratio (a measure of tendency to adsorb at the interface relative to that to form micelles in bulk phase).[1b] The chemical structures of **1** and **2** are shown in Figure 1, together with those of a comparable cationic gemini surfactant, ethanediyl-1,2-bis(dodecyldimethyl-

* Corresponding author. Tel: 04-7124-1501 (ext. 3663). Fax: 04-7122-1442. E-mail: ktsubone@rs.noda.tus.ac.jp.

† Faculty of Science and Technology.

‡ Institute of Colloid and Interface Science.

(1) Rosen, M. J. *Surfactants and Interfacial Phenomena*, 3rd ed.; Wiley-Interscience: New York, 2005. (a) pp 415−427. (b) 149−157. (c) pp 127. (d) pp 60−64. (e) p 215.

(2) Rosen, M. J. *CHEMTECH* **1993**, *30*, 23.

(3) Summers, M.; Eastoe, J.; Davis, S.; Du, Z.; Richardson, R. M.; Heenan, R. K.; Steytler, D.; Grillo, I. *Langmuir* **2001**, *17*, 5388.

(4) Dufour, M.; Guyot, A. *Colloid Polym. Sci.* **2003**, 97.

(5) Green, B. W.; Sheetz, D. P. *J. Colloid Interface Sci.* **1970**, *32*, 96.

(6) Liu, J.; Chem, C. H.; Gan, L. M.; Teo, W. K.; Gan, L. H. *Langmuir* **1997**, *14*, 4988.

(7) Boisson, F.; Uzulina, I.; Guyot, A. *Macromol. Rapid Commun.* **2001**, *22*, 1135.

(8) Gerber, M. G.; Walker, L. M. *Langmuir* **2006**, *22*, 941.

(9) Zhu, Z.; Gonzalez, Y. I.; Xu, H.; Kaler, E. W.; Liu, S. *Langmuir* **2006**, *22*, 949.

(10) Kunitake, T.; Nagai, M.; Yanagi, H.; Takarabe, K.; Nakashima, N. *J. Macromol. Sci. Chem.* **1984**, *A21*, 1237.

(11) Akbay, C.; Gill, N.; Powe, A.; Warner, I. M. *Electrophoresis* **2005**, *26*, 415.

(12) Pindzola, B. A.; Jin, J.; Gin, D. *J. Am. Chem. Soc.* **2003**, *125*, 2940.

(13) Hamid, S. M.; Sherrington, D. C. *Polymer* **1987**, *28*, 325.

10.1021/la060156y CCC: $33.50
Published on Web 08/23/2006